



**UNIVERSITY OF
KWAZULU-NATAL**

**INYUVESI
YAKWAZULU-NATALI**

**REAL-TIME MODELLING AND SIMULATION OF DISTRIBUTION
SYSTEM PROTECTION WITH AND
WITHOUT RENEWABLE DISTRIBUTED GENERATION**

By

Ntuba Irene Nkhasi

211535371

In partial fulfilment of the academic requirements for the degree of

Master of Science in Electrical Engineering,

College of Agriculture, Engineering and Science

University of Kwazulu Natal

December 2017

Supervisor: Dr A K Saha

ABSTRACT

The conventional radial power distribution systems were initially not designed to accommodate distribution generation (DG). As DG penetration is being considered by many distribution utilities, there is a rising need to address many incompatibility issues that put a big emphasis on the need to review and implement suitable protection schemes. For a significant greenhouse gas reduction using photovoltaic systems, numerous generators ought to be embedded in the distribution system. For an effective penetration of PV systems on a large-scale into the current distribution network, considerable work to investigate the nature of incompatibility problems has been done and research is being carried out to develop successful integration strategies. The main objectives of the thesis are; to model and simulate a distribution system protection scheme, to study radial networks' protection system challenges after embedding distributed generation sources, investigation on the impacts of high PV penetrations on protection systems of distribution networks and lastly make modification recommendations and essential review process of existing protection equipment settings. To accomplish the above-mentioned objectives, a radial distribution network is modelled, simulated and protection settings validated. The PV generation system is designed and added to specific distribution feeders and steady steady-state results obtained. The results show that addition of DGs cause the system to lose its radial power flow. There is an increase in fault contribution hence causing maloperation such as protection coordination mismatch. An overall protection scheme is then proposed based on the addition of DG's and an efficient adaptive protection system for the distribution networks with a considerable penetration of dispersed generations implemented. The impact study is performed which is compared with the existing protection scheme and necessary modifications done. The entire analysis is simulated on a real-time digital simulator (RTDS) and results displayed in a MATLAB environment. For the islanded mode, relaying considerations are provided and implementation of anti-islanding techniques achieved.

Acknowledgements

My heartfelt gratitude goes to my supervisor Dr. A.K Saha for his constant supervision, valuable academic support and patience during the course of the research. Thanks for the encouragement and always being available to guide and advice although it was long and went through some bumpy times. It has been an absolute pleasure working under his selfless supervision. My sincere appreciation also goes to my friend N.V. Ndlhozi, who dedicated time off his busy schedule and work to proofread my drafts. To my mother and family, thank you for your encouragement and support all the way through my research journey, thanks for not letting me give up. Finally yet importantly, this thesis is a dedication to my late father and sister who are not around anymore to witness my academic achievements, this one is for you.

Table of Contents

ABSTRACT.....	ii
Acknowledgements.....	iii
List of Figures:.....	vii
List of Tables	ix
List of Abbreviations:	x
1. Introduction	1
1.1. Background	1
1.2. Importance of research	2
1.3. Research objectives	3
1.4. Research scope and limitations	3
1.5. Problem statement	4
1.6. Thesis outline	4
2. Literature Review	6
2.1. Introduction	6
2.2. Review on faults.....	6
2.3. Protection philosophy.....	7
2.3.1. Essential qualities of protection.	8
2.4. Protective equipment.....	8
2.5. Protection scheme	9
2.5.1. Transformer protection	10
2.5.2. Differential protection.....	10
2.5.3. Overcurrent Protection.....	10
2.6. Protection coordination	12
2.7. Distributed generation	12
2.7.1. Distributed Generation Technology.....	13
2.7.2. Grid-tied Photovoltaic System.....	13
2.8. Impact of DG integration to the existing grid and protection scheme	14
2.9. Mitigation methods to DG penetration issues.	16
3. Methodology.....	18
3.1. Software selection	18
3.2. Modelling of the distribution network in RSCAD	19
3.2.1. Draft programme.....	19
3.2.2. Runtime programme	19

3.3.	Protection set-up.....	20
3.4.	Protection relay testing.....	20
3.5.	PV generation system design	20
3.6.	Grid-tied inverter model development	21
3.7.	Stand-alone grid tied PV system	21
3.8.	Optimal relay coordination.....	21
3.9.	PV impacts mitigation methods	22
3.10.	Recommendation for future works	23
4.	Modelling and real-time simulation	24
4.1.	Test distribution system configuration.....	24
4.2.	System full load conditions	25
4.2.1.	Fault and breaker logic control	27
4.2.2.	Relay logic control.....	27
4.3.	Software relays' simulation:.....	28
4.3.1.	Testing software Relay-3	28
4.3.2.	Time setting of Relay-2:	29
4.3.3.	Testing software Relay-2:	30
4.3.4.	Time setting of Relay-1:	31
4.3.5.	Testing software Relay-1:	31
4.3.6.	Testing software Relay-4	32
4.4.	Protection Coordination results	33
5.	Experimentation and Verification	37
5.1.	Hardware-in-loop simulation	37
5.1.1.	Testing Hardware Relay-3	38
5.1.2.	Testing Hardware Relay-2	38
5.1.3.	Testing Hardware Relay-1	38
5.1.4.	Testing Hardware Relay-4	39
5.2.	Grid-connected PV system.....	40
5.2.1.	Inverter model development	41
5.2.2.	Steady-state operation.....	43
5.2	Overcurrent Protection set-up	48
5.3	Islanding Protection.....	52
5.3.2	Passive techniques	52
5.3.3	Active techniques.....	53

5.3.4	Islanding operation.....	53
6	Conclusion.....	57
	References.....	59
	Appendix.....	65

List of Figures:

Figure 1: Single line diagram of the modelled distribution system	24
Figure 2: System R.M.S Currents	26
Figure 3: Distribution system RMS voltages	26
Figure 4: Fault and circuit breaker logic	27
Figure 5: Software overcurrent relay used	28
Figure 6: Relay-3 operating for a fault on 380 V busbar	29
Figure 7: Relay-2 testing for a fault at zone-3 (380V busbar)	30
Figure 8: Relay-2 operating for a fault at zone-2 (11 kV busbar)	30
Figure 9: Relay-1 operating for a fault at zone-2 (11 kV busbar)	31
Figure 10: Relay-1 operating for a fault at zone-1(132 kV busbar)	32
Figure 11: Relay-4 operating for a fault on the 22 kV busbar	32
Figure 12: Relay-2 failing to operate	33
Figure 13: Failure of relay-3 and relay-2 to operate	34
Figure 14: Operation of relay-2 for a fault at protection zone 3	35
Figure 15: Relay-4 failing to operate	35
Figure 16: System hardware-in-loop connection	37
Figure 17: Hardware Overcurrent Relay 3 operating	38
Figure 18: Hardware Overcurrent Relay 2 operating	38
Figure 19: Hardware Overcurrent Relay 1 operating	38
Figure 20: Hardware Overcurrent Relay 4 operating	39
Figure 21: RSCAD model of grid connected PV system	40
Figure 22: Large and small time-step simulation interface	42
Figure 23: Characteristic curves of the PV array at STC	43
Figure 24: PV Array output voltage	43
Figure 25: Stand-alone PV System output RMS voltage	44
Figure 26: Single line diagram of the grid-tied photovoltaic system	45
Figure 27: Grid-connected PV system voltages	45
Figure 28: Grid-connected PV system CTs secondary RMS current	46
Figure 29: PV System RMS voltage	47
Figure 30: System RMS currents	47
Figure 31: Relay-3 testing	50
Figure 32: Relay-2 testing	50
Figure 33: Testing relay-1	51
Figure 34: Relay-4 testing results	51
Figure 35: A radial feeder with PV generation integrated	53
Figure 36: Distribution system currents due to islanding	54
Figure 37: Protection against islanding layout	54
Figure 38: Circuit breaker logic	55
Figure 39: Circuit breaker 1 and 6 opening on fault F-1 occurrence	55
Figure 40: System line current during islanding protection	56
Figure 41: Circuit breaker 1 and 6 opening on fault F-2 occurrence	56
Figure 42: Distribution System Model on RSCAD environment	65

Figure 43: GTFPI and GTAO card used for exporting signals.....	66
Figure 44: PV System characteristics graphs.....	66
Figure 45: Maximum Power Point Tracking control circuit.....	67
Figure 46: 2-level DC/AC inverter and filter.....	67
Figure 47: Triangle wave data generator for the DC/AC inverter	67

List of Tables

Table 1: Transformers, load and source parameters	25
Table 2: Voltages and Currents measured on the distribution system.....	25
Table 3: Comparison of operating time from software and hardware relays	39
Table 4: Parameters of Mitsubishi Electric Photovoltaic Module	40
Table 5: PV system parameters and expected outputs at STC.....	42
Table 6: PSM and a values	49
Table 7: Dial output and corresponding fault	65
Table 8: 1st iteration (Slack variables as basics)	68
Table 9: 2 nd iteration (X2 enters as basic, S2 comes out)	68
Table 10: 3 rd iteration (X1 enters as basic, S1 comes out).....	68
Table 11: 4 th iteration (X3 enters as basic, S5 comes out).....	68

List of Abbreviations:

DG	Distributed Generation
IEEE	Institute of Electrical and Electronics Engineers
IEC	International Electro-technical Commission
PV	Photovoltaic
DC	Direct Current
AC	Alternating Current
RTDS	Real-time Digital Simulator
CT	Current Transformer
VT	Voltage Transformer
CB	Circuit Breaker
OCR	Overcurrent Relay
TMS	Time Multiplier Setting
IDMT	Inverse Definite Minimum Time
PSM	Plug Setting Multiplier
CTI	Coordination Time Interval
LOM	Loss of Mains
ETAP	Electrical Transient and Analysis Program
PSCAD	Power System Computer Aided Design
HVDC	High Voltage Direct Current
HIL	Hardware-in-Loop
GUI	Graphical User Interface
GTFPI	Gigabit-transceiver Front Panel Interface
GTAO	Gigabit-transceiver Analogue Output
MPPT	Maximum Power Point Tracking
RMS	Root Mean Square
VSC	Voltage Source Converter
IGBT	Insulated Gate Bipolar Transistor
STC	Standard Test Conditions
NOCT	Normal Operating Cell Temperature
PCC	Point of Common Coupling
LPP	Linear Programming Problem

1. Introduction

This research work highlights the effective use of a real-time digital simulator (RTDS) for modelling, analysis and protection of an electrical distribution network emanating from a 132 *kV* grid. It provides an introduction to overcurrent protection scheme on a distribution network injected with dispersed generation (DG) and the DG potential benefits to distribution utilities discussed. A review of the protection issues associated with dispersed generation is conducted. In this chapter, the research background, objectives and methodologies employed in this thesis are stated and finally the chapters outline is provided. The system under study is a modified adaptation of the IEEE test feeders.

1.1. Background

Due to a constantly rising energy demand and roughly two centuries of total dependency on fossil fuels, the world has begun to feel the greenhouse gas emissions effect. As the demand for electrical energy seems to be on a rise, alternative fuels are being looked at apart from fossil fuels that power thermal power plants. Nuclear or hydroelectric power generation systems do not generate greenhouse gases and are another alternative to be considered except that a high level of safety is required for nuclear while water levels, which hydroelectric depend on, are not entirely reliable [1] [2].

Distributed generation systems such as photovoltaic energy, wind turbines, fuel cells and other energy storage technologies are at present increasingly finding their significance to solve environmental issues. Unlimited renewable energy resources such as solar can serve as substitutes for fossil fuels consequently reducing greenhouse gases significantly. Photovoltaic generation through photovoltaic effect, converts solar irradiation directly into electrical energy using solar cells. With the technical evolution, finance and electrical markets expansion, new technologies make possible the electricity generation in small plants closer to consumers.

This new concept leads to the development of innovative electrical power distribution systems where photovoltaic (PV) generation systems supplies some of the energy and centralized generation produces some. Traditional distribution systems are of radial topology, which only permits flow of power in a single downstream direction and the protection schemes are dependent on this assumption, particularly overcurrent relay selectivity and coordination [3]. The unidirectional power flow assumption does however not hold when

distributed generation is injected in the distribution system. Back flow of current occurs due to multiple sources hence disturbing the standard overcurrent protection and their relay sequential operation.

Major concerns relating to penetration of PV systems include poor relay coordination, sympathetic tripping and unintentional islands which result from continuous power flow from the dispersed generation systems although the grid is disconnected due to a fault. Many power distribution utilities currently mitigate these problems by limiting the DG units' capacity and using strategic location [4]. This thesis aims to focus on the modelling of a radial distribution feeder system structure and study the impacts of distributed energy resources when integrated with distribution systems including relaying considerations when in islanded mode.

1.2. Importance of research

For any nations' technological and economic progression, a steady and reliable electric power supply system is an inevitable pre-requisite. It is a known fact that around the world a higher percentage of the power systems' equipment damage and customer service interruptions results from failure and faults in the electricity distribution feeders since overhead distribution systems are subject to either temporary or permanent faults. Distribution systems comprise of many diverse and expensive items that require a substantial capital investment and it therefore it is very essential to protect this equipment. Moreover, a considerable quantity of photovoltaic generators has to be injected into the distribution network for a significant reduction in the greenhouse gas emissions. Large-scale PV penetration however gives rise to potential distribution system protection problems such as protective equipment coordination issues, etc. [3]. For an effective penetration of PV systems on a large-scale into the current distribution network, considerable work to investigate the nature of incompatibility problems has been done and this research is being carried out with a purpose to develop and implement strategies for successful integration of PV generators into the present network. The thesis aims to cover a systematic approach from modelling the distribution network to various protective devices' coordination on different nodes of the feeder, the DG's impact on the system and to cover lastly the implementation of mitigation methods on the identified issues.

1.3. Research objectives

The core objectives of the thesis are:

- Modelling and simulation of a distribution system overcurrent protection scheme
- To introduce PV generation system into the distribution network and identify issues arising concerning the network protection system.
- To address the identified and aforementioned issues to maintain and improve the grid-tied photovoltaic energy systems' performance.
- To investigate the impact of high PV penetrations levels distribution system stability and on protection systems performance while varying the PV point of common coupling to different voltage levels.
- To make modification recommendations and essential review process of existing protection equipment settings for correct discrimination.
- To implement mitigation strategies to some of the problems arising from introduction of PV systems to the distribution network
- To make recommendations on studies that can be carried out to further this research work

1.4. Research scope and limitations

The research identifies issues related to interconnection of PV systems to distribution utilities, reviews and implements some pragmatic mitigation methods. This research scope and limitations are as follows:

- Only the major technical issues with over-current protection relays' coordination of a distribution system are covered and addressed.
- The DG technologies have been limited to photovoltaic (PV) generation, which are based on solar panels and DC-AC inverters.
- The main focus is on protection scheme and protection issues related to interconnection of the PV system.
- Models have been developed in RSCAD and RTDS simulator and some of the standard models available in the software have been used.

1.5. Problem statement

To demonstrate by simulation and experimental tests a distribution system model and overcurrent protection scheme implementation and testing of protection devices through a hardware-in-loop connection. As outlined earlier, the electricity demand is currently fast growing and power engineers are bound to produce electricity from renewable energy sources to overcome this upsurge and simultaneously diminish environmental effects and carbon footprint of power generation. To address mitigation methods to some of the issues created by addition of distributed generation to electricity distribution network.

1.6. Thesis outline

This section presents an overview of the research work covered. The thesis consists of six chapters and an appendix. Each chapter's summary of content is provided and organized below as follows:

Chapter 1: Introduction

This is an overview to the research work undertaken, outlining aims and objectives, description of motivation, research scope plus limitations and the background of this research. It introduces the concept and background of distributed generation, existing methods of harnessing renewable energy, particularly the role of photovoltaic systems in this perspective and the drawbacks of connecting DGs on the existing protection systems.

Chapter 2: Literature Review

This section reviews the existing literature on distribution systems overcurrent protection schemes followed by a discussion the several types and nature of dispersed generation technologies with distinct reference to inverter tied PV systems. The impacts of grid-tied PV systems on distribution networks are discussed, focusing mainly on feeder protection problems due to interconnection of DG systems. It also highlights in theory some of the mitigation methods to the negative impacts. A comprehensive understanding of the research problem has been presented and the published research work results discussed in detail.

Chapter 3: Methodology

The chapter outlines a systematic approach deployed in this research to achieve objectives discussed in the introduction. It gives briefly an overview to overcurrent protection techniques and describes the type of simulator used, its main features and advantages pertaining to the research work.

Chapter 4: Modelling and real-time simulation

In this chapter, the distribution network and overcurrent protection scheme for the radial feeder is modelling and implemented. The chapter contains designed models in the graphical user interface (RSCAD) environment; it also consists of several outcomes from investigations taken up as a section of the research. It presents model calculations and tables for some of the relevant algorithms employed in the study. The distribution network is analysed and protection system coordination implemented, with which results obtained serve as a basis that results after modifications and interconnection of DGs are compared to.

Chapter 5: Experimentation and verification

All results obtained from the software simulations are verified by substituting the software relays on the network with the hardware relays through a hardware-in-loop connection. Since probable problems generated by DG's addition to distribution networks include protective device discrimination and possible formation of islanded systems, the test radial distribution feeder topology is then modified by introducing PV generation at nodes on the network and a detailed analysis of the simulation results done to understand the PV generation impact on protection coordination. A solution to overcome the issues is implemented and simulation results with different DG interconnection points and configurations are presented.

Chapter 6: Conclusion

This chapter recapitulates the research work outcomes and key results as well as some recommendations for future work. A detailed discussion of the research work results and a comprehensive understanding of the problems has been presented.

2. Literature Review

2.1. Introduction

The diminishing of fossil fuels and increasing environmental awareness is resulting in an increasing distributed power generation worldwide [5]. On the other hand, the scarcity of fossil fuels, their increasing costs, the limited investment on new large power plants and transmission lines construction are the other reasons contributing to the deployment of small power plants which can be connected to strategic points on distribution systems or close to load centres [6]. The continuing increase in the penetration of distributed generation (DG) and the adoption of active network-management solutions in distribution networks across the world creates a network protection challenge due to the effects on fault levels, fault current paths, etc. [7].

Distribution systems are generally designed to operate without any generation on the distribution network or customer loads. Due to the accumulating number of DG connected to distribution networks, there arise concerns regarding power quality, reliability, protection devices and control of the utility system [8]. Since integration of distributed generation in distribution networks imposes many challenges, distribution overcurrent protection has become more important today than it was a decade ago [9]. The distribution system protection has faced new challenges due to distributed generation, which may be successfully accomplished through the combination of the existing protections, such as overcurrent protection, with modern protections based on evolving technologies discussed in [10].

2.2. Review on faults

Electrical networks, machines and equipment are often subjected to various types of faults while in operation. Current that flows through the distribution is the element with which detection of faults can be done given the large increase in current flow during short circuits. The fault inception also involves insulation and conducting path failures, which result in short and open circuit of conductors. Faults could either be symmetrical or asymmetrical; symmetrical faults being the ones with which all lines are affected simultaneously and with asymmetrical, either one or two phases are affected [11]. With respect to overcurrent protection on distribution systems, various types of currents such as overload current, short circuit current and ground fault current are taken into consideration. Overload currents result from a number of factors such as successive outages of power devices, insufficient available

component capacity and incorrect operation. With short circuit, the effects are not limited to the region of exposure as they could influence the performance of remote equipment as well.

The effects of fault currents include mechanical stress, undesirable overheating, deterioration of insulation, etc. [12]. Equipment that are frequently exposed to short circuit conditions are, therefore, very likely to fail as a result of such stresses. In terms of reliability, the failure rate of these equipment will increase with time. The majority of faults that occur on a power system involve ground and occur between conductor and tower. Large grounded distribution systems are subject to system faults near the stations that produce extremely high fault currents. These high currents may inflict severe circuit breaker interrupting duties and stress on system equipment. The reduction of ground current is rapid as the fault distance increases from the source; therefore, the most severe faults are those within a few miles of the station [13] .

2.3. Protection philosophy

Power distribution systems are subjected to constant disturbances caused by arbitrary load changes, faults created by natural causes and at times due to equipment or operator failure [14]. If a fault occurs in an element of the network, an automatic protective device is needed to clear the fault in a fraction of seconds to keep the healthy section of the system in normal operation and to isolate the faulty element as quickly as possible [15]. Faults that persist longer on a system may cause damage to some vital sections due to fire that may result from heavy short circuits and as a result, the system voltages may decrease causing loss of synchronism of the system machinery and equipment.

The main objectives of distribution system protection are [11] [16]

- To disconnect faulted lines, transformers, or other apparatus.
- To limit service outages to the smallest possible segment of the system.
- To minimize the duration of a fault on the distribution network.
- To eliminate safety hazards as fast as possible.
- To protect the consumers' apparatus.
- To protect the system from unnecessary service interruptions and disturbances.

Protective systems include relays, circuit breakers and transducers that function together to isolate the faulty section from the healthy sections of system. Circuit breakers work to

disconnect the faulty section of the system when triggered to do so by the relay which detects, locates a fault and sends a command to the disconnection circuit breaker [15]. The relay constantly monitors electrical quantities of the system which differ during abnormal conditions. Protective relays do not foresee or prevent the occurrence of a fault, they only take action after a fault has occurred [17] .

2.3.1. Essential qualities of protection.

The protection arrangements for any network must take into account and adhere to the following basic requirements:

- a) **Selectivity**: also known as discrimination, refers to the ability to maintain continuity of supply by disconnecting the minimum section of the network necessary to isolate the fault and the remaining healthy sections left intact [15] [11] [18].
- b) **Reliability**: refers to the ability of protection to operate correctly. It consists of two elements being dependability and security, which are the certainty of a right operation on the occurrence of faults and the ability to avoid incorrect operation during faults respectively [11] [19]
- c) **Sensitivity**: the protective relay should be sufficiently sensitive to the magnitude of the current and to operate when the current just exceeds the pre-set detection threshold known as the pick-up current [15].
- d) **Stability**: the ability of the protective system to remain stable even when a large current is flowing through its protective zone due to an external fault which does not lie in its zone. The fault is cleared by the concerned circuit breaker [19].
- e) **Speed**: a protective system should quickly isolate the faulty element as quick as possible to maintain system stability and minimise damage to the equipment.
- f) **Economics**: achieving maximum protection at the lowest cost as possible, which usually should not be more than 5% of the total cost of the power system being protected [18] [19].

2.4. Protective equipment

The ability of protective equipment to minimize damage when failures occur and reduce service interruption is needed not only for economic reasons, but also for reliability of service to the public in general. Distribution system overcurrent protection is generally accomplished by use of protection transducers that include current transformers (CTs), voltage transformers

(VTs), circuit breakers and overcurrent relays [20] [21]. The protective equipment collectively functions to detect and isolate only that particular part of the network responsible for the fault.

a) Voltage transformers

According to Sleva [22], voltage transformers accurately reflect primary network voltage into the secondary low-voltage winding and are connected in shunt with the distribution system components. They are used to provide lower input signals to the protective relays and to physically isolate the relays and other instruments from the high voltages of the network. The VTs' secondary windings standard voltage rating is 110 V line to line.

b) Current transformers

Current transformers step down high currents to low values that are suitable for the operation of relays and other measuring instruments [23]. The standard current ratings of CTs used in practice are 5 A or 1 A. They are designed to withstand fault currents as high as 50 times the full load currents for a few seconds.

c) Circuit breakers

Circuit breakers (CBs) are fault-interrupting devices that enable or interrupt the flow of current to power system components. They separate the faulty parts from the rest of the grid safely and reliably to avoid endangering unaffected parts and equipment [24]. The circuit breakers are not self-actuating; they do not have their own tripping intelligence hence they are used in conjunction with relays and only function when a trip or close signal is received.

d) Relays

Protection relays form the most important part of the protection scheme, as a result, their capability and functionality plays a significant role in how the protection scheme works [22]. They serve as decision-making elements triggered by current and voltage measurements obtained from the voltage and current transformers. If the magnitudes of the incoming signal are outside a pre-set threshold, the relays operate generally to either open or close electrical contacts to initiate some further operations such as tripping of a circuit breaker [11] [15].

2.5. Protection scheme

It is usually difficult to define precisely the protection scheme that should be adopted for an electricity distribution system, given the large number of valid alternatives for each situation. However, any protection scheme should strike a balance between the technical and economic aspects to avoid use of sophisticated protection devices for small machines or less important

system elements [11]. Protection schemes are designed to detect abnormal network conditions, normally contingency-related, and initiate pre-planned, corrective measures to mitigate the consequence of the abnormal condition and provide acceptable system performance [25]. They include one or more relays of the same or different types. The following are some of the most common protective schemes usually used in modern power systems [15].

2.5.1. Transformer protection

When large transformers fail, there is a high possibility of consequential damage due to tank rupture with an oil spill and fire that spreads to the surrounding area. To minimize the damage, transformer sudden pressure and differential relays are employed to quickly detect and isolate the faulty transformer [22]. Nowadays the transformer differential protection resides in microprocessor-based relays, which execute signal processing, filtering, currents compensation, and computation of differential and restraint currents. The relay providing transformer differential protection is normally linked to the current transformers from both transformer windings [26].

2.5.2. Differential protection

Differential protection is a method that functions when the vector difference of two or more similar electrical magnitudes exceeds a predetermined value. The principle is founded on the direct application of Kirchhoff's first law [27] [28]. An internal fault is identified by comparing the electrical conditions at the terminals of the equipment to be protected in a method. The main component of differential protection scheme is the differential relay that operates when the phasor difference of similar electrical quantity exceeds a set value. Differential protection is also referred to as unit protection since it is confined to protecting a particular unit or equipment of a plant or substation [15].

2.5.3. Overcurrent Protection

Overcurrent protection is a method used for detecting excessive currents in a system and cutting the delivery of further current into the system when overcurrent is detected [29]. Very high current levels in electrical distribution systems are usually a result of faults on the system. These high fault currents can be used to determine the presence of abnormalities on the distribution network and operate protection devices, which can vary in design depending on accuracy and complexity required [11]. Among the more common types of protection

devices are thermomagnetic switches, moulded case circuit breakers, fuses and overcurrent relays. Overcurrent relays are the most common form of protection devices used to deal with excessive currents on electricity distribution networks [11].

2.5.3.1. Time overcurrent protection

To guard against the possible failure of main protection devices in a distribution system, time overcurrent protection relays usually function as backup protection to prevent the system from experiencing catastrophic consequences [30]. The relays and their variants represent the largest installed base of protective equipment on any distribution systems and may be considered as the backbone of any protection strategy. The microprocessor-based relays possess algorithms for monitoring the system through current and voltage inputs from CTs and VTs respectively [31] [32].

Overcurrent protection methods directly use the magnitude of the current as indicator that a fault has occurred and trip if the measured current overcomes a certain threshold [33]. The relays operate within a time, inversely proportional to the fault current. The fault current magnitude near the source is higher and hence the shortest tripping time [8]. Due to the impedance between the two points, the fault current magnitude at the far end of the line is relatively less and results in longer tripping time. This brings the flexibility on operation of local protection devices to clear first. According to IEEE Std. C37.112-1996, inverse time overcurrent protection generally uses the following standard characteristic equation:

$$t_{op} = \frac{0.14}{PSM^{0.02-1}} \times TMS \quad (1)$$

where; $PSM = \frac{I_{relay-coil}}{I_{pick-up}}$, t_{op} = time of operation, TMS = time multiplier setting and $I_{pick-up}$ = pick up current .

The standard inverse time characteristic equation is usually used for line protection, very inverse time characteristic equation used when the short-circuit current of close-up fault is much greater than far end fault and the extremely inverse time characteristic equation suitable for over-thermal protection caused by heavy load currents [34]. With inverse definite time overcurrent IDMT relays, the pick-up current is taken as 1.2 to 2 times the full load current, in steps of 0.05. The time dial setting (TMS) defines the operation time of the device for each current value [32].

2.6. Protection coordination

With protective relays, the aim is to achieve coordination between the downstream and upstream relays and circuit breakers [32] [21] [35]. The goal is to allow enough time for the relay and breaker closest to the fault to clear the fault from the system before the backup relay associated with the adjacent section to the source could initiate the opening of its circuit breaker. The time interval allowed between two adjacent relays' operation in order to achieve correct discrimination between them is called the grading margin. Taking into consideration factors such as circuit breaker operating time, relay overshoot time, contact gap together with relay and CTs errors, the MiCOM relay user manual shows that a time grading margin of 400 *ms* is used.

An undesirable occurrence known as over-trip often happens, a situation whereby a feeder relay and supply-side relay both trip for the same feeder fault and is usually blamed on poor relay coordination. The relay and breaker nearest to the point of fault must be able to see the fault and operate before other relays in the system, so that healthy parts of the system will not be interrupted [35]. One of the important coordination problems on distribution feeders is the proper selection of protective devices for correct sequential operation. Protection of distribution lines can be provided in many different ways. A survey of industry practices in the protection of distribution circuits showed that a large percentage of utilities employ phase and ground overcurrent protection for instantaneous tripping of temporary faults with time delayed tripping for permanent faults [36].

2.7. Distributed generation

According to Borbely and Kreider [37], distributed generation is not entirely a new concept because originally, all energy was produced and consumed at or near the process that required it. In relation to them, a fireplace, wood stove, candle, alarm clock and car battery are all forms of small scale, demand-sited "distributed" energy. Distributed generation is therefore a new concept in the economics literature about electricity markets, but the idea behind it is not new at all [38]. A number of terms have emerged to define power that comes from sources other than from large, centrally dispatched generating units connected to a high-voltage transmission system or network [39]. The term distributed generation can be used interchangeably or considered synonymous with embedded generation and dispersed generation, which are now barely used.

Motivated by environmental concerns, the necessity to diversify energy sources, energy autonomy and efficiency, the penetration of distributed generation from renewable resources like solar and wind is rapidly growing as the trend moves away from large centralized power stations towards more meshed power distribution on the electricity grid [40]. Distributed generation is commonly thought of as small-scale generation that is used onsite and/or connected to a distribution network [39]. The type of technologies employed have historically varied, but were generally limited to small engines or combustion turbines fuelled by diesel, gasoline, or natural gas and also costly to run relative to grid supplied power [39]. More recently, intermittent renewable resources such as solar, small hydro, and wind energy are thought of as distributed generation being deployed to reduce overall emissions [41].

2.7.1. Distributed Generation Technology

This section considers the technology deployed in the generation of electrical power from the sun (solar energy) as a typical example of distributed generation technology. The choice of this source without any prejudice to other sources such as wind, micro-turbines, fuel cells, geothermal and internal combustion engines is because of its relevance to the study.

With reference to [42], solar energy could be used to describe any phenomenon that is created by solar sources and harnessed in the form of energy, directly or indirectly – from photosynthesis to photovoltaics. According to Langston and Ding [43], the direct conversion of sunlight into an electrical energy is achieved by a process called photovoltaic (photo = light, voltaic = electrical potential) effect. Although solar energy is the most abundant energy resource, only an infinitesimal fraction of the available solar energy is used [44]. Luo and Ye [44], state that the amount of solar energy reaching the earth surface is so vast that in one year it is about double as much as will ever be obtained from all of the planet's non-renewable resources of coal, oil, natural gas, and mined uranium combined. Therefore, solar energy consequently appears to be an easy alternative next to conventional sources, like electricity, coal and other fossil fuels.

2.7.2. Grid-tied Photovoltaic System

Photovoltaic (PV) energy has grown at an average annual rate of 60% in the last five years, exceeding one third of the cumulative wind energy installed capacity, and is becoming a significant part of the energy mix in some regions and power systems [45]. Several studies [45] [46] [47] [48], show that it is driven by a reduction in the cost of PV modules, environment friendliness, containing no rotating elements and it being an inexhaustible

source. Recently, energy generated from clean, efficient and environmentally friendly sources has become one of the major challenges for engineers and scientists and therefore photovoltaic (PV) application has been a subject of interest in research since it appears to be one of the most efficient and effective solutions to this environmental problem [47]. Compared to stand-alone systems, grid-connected PV systems account for more than 99% of the PV installed capacity. In grid-connected PV systems, the power generated by the PV plant is uploaded to the grid for direct transmission, distribution, and consumption [49].

PV arrays are built up of combined series or parallel combinations of PV solar cells [48]. The PV cells generate a direct current (DC) that is significantly dependant on the solar irradiance, temperature, and voltage at the PV system terminals. This DC power is transformed and interfaced to the grid via a PV inverter [45]. At a certain environmental condition, one unique operating point exists to provide the PV generation system with maximum output power. PV modules exhibit non-linear voltage-current characteristics, and the maximum power point varies with the irradiation and temperature [47].

2.8. Impact of DG integration to the existing grid and protection scheme

Conventional distribution networks are generally arranged in radial topology and the protection strategies in use assume single source in-feed and radial flow of current [6] [50]. Conti [51] shows that the introduction of DGs affects several operational aspects of AC power systems including their protection philosophy. If the PV penetration is high, PV systems can subject the grid to several negative impacts. The following paragraphs discuss some of the main issues associated with the protection of AC distribution system embedding DGs.

a) Varying fault level contribution

Penetration of DGs can influence the performance of a current-based protection scheme by changing the fault current seen by the protective device [6] [52]. Nuisance tripping can result if the current measured exceeds the relay's pick-up setting. The current that flows into a fault can come from three sources on a distribution network: namely, in-feeds from the transmission system, in-feeds from distributed generation or in-feeds from loads with induction motors. DG connection causes fault levels close to point of connection to increase, which is caused by an additional fault level from the generator and can cause the overall fault level to exceed the designed fault level of the distribution equipment.

The risks when fault levels are exceeded will cause damage and failure of the plant, with consequent risk of injury to personnel and interruption to supplies. Different distributed generation technologies come with varying fault level current contribution and provision needs to be made for adequate system protection under all system configurations. The situation may lead to protection discrimination problems and impose requirements for switchgear and potentially other plant capacity upgrade and/or reinforcement.

b) Loss of mains

One of the most important network safety requirements when local generation is present at the distribution level is the loss of mains (LOM) protection, which has been recognised as one of the most challenging aspects relating to distributed generation [53]. Loss of mains (or islanding) occurs when part of the public utility network or a portion of the distribution system becomes electrically isolated from the remainder power system, yet continues to be energized by DG connected to the isolated subsystem.

Due to opposite current flow from DG, the reach of a relay is shortened, leaving high impedance faults undetected. If LOM is not detected, then the generator could remain connected, causing a safety hazard within the network. When a utility breaker is opened, a portion of the utility system remains energised while isolated from the remainder of the utility system, resulting in injuries to the public and utility personnel [35] [36]. In history, up until not long ago, loss of mains protection was put to use mainly to protect from the viewpoint of ensuring personnel and public safety since there was little DG in the system.

c) Protection coordination disruption

Since the initiation of electrical systems, coordination tasks were performed to ensure that protection systems would operate with the necessary reliability and security. DG connection to a distribution feeder can also change power flow and fault current direction, consequently disrupting the coordination amongst the protection devices as they are mostly non-directional units. Protection coordination is employed for cases such as security against failure or incorrect relay/device operation. Due to one source of power, the relays can be non-directional since the current flows in one direction, but the injection of distributed generation poses a threat to the coordination system because the generators also contribute to the total fault current [54].

At the end of a distribution feeder protected by a standard time graded overcurrent protection scheme, a problem of discrimination appears when additional generation is connected at the far end of the feeder and thereby results in downstream protection seeing fault current. Also, the connection of distributed generators to the distribution lines raises challenges for the effective settings for the feeder protection since the protective system should as well be designed with due regard for its own unreliability. That is installation of backup protective systems to operate in case of primary equipment failure [22].

2.9. Mitigation methods to DG penetration issues.

As the penetration of DG increases, grid flexibility requirements also increase. The previous sections have presented the status of and major obstacles to the establishment of DG within utility systems. The following are some potential solutions that have been discussed and recommendations directed towards injection of DG.

a) Modifying the existing system

When fault level exceeds the current design limits because of distributed generation installation, upgrading the capability of existing equipment such as circuit breakers is an option to enhance the fault level capabilities of the distribution system [55]. This method is widely used throughout the world as a solution to the issue of increased fault levels. To avoid control interactions among several DG units and their controllers, in large distribution networks, some precautions such as keeping a minimum distance among DG plants and coordinating controllers should be taken [56].

b) Utilizing Fault Current Limiters (UFLs)

In [55], it is discussed that UFLs are devices that limit the fault current by increasing the system impedance. During faults, the resistances increase very quickly and sharply for high fault currents consequently reducing the current to low and acceptable limits.

c) Limiting the Inverter Current

Under the fault conditions, blocking the DG inverter is an extensively used strategy in order to protect the inverter from the high fault currents and reconnect them when normal operation has been restored [55].

d) Adaptive Overcurrent Protection

One method that can be utilized is the directional overcurrent relay with dynamic settings. This method needs fast and effective monitoring of system conditions. It will automatically update relay settings based on prevailing system conditions [57].

e) Distance and Directional Comparison Protection

Even with obvious advantages of better and simpler downstream coordination, fixed reach zone and relative immunity to the source impedance behind the protection relay, distance protection was not considered at the radial feeders [57]. However, nowadays many utilities are applying this protection at the distribution level due to distributed generation. Owing to distributed generation penetration, the fault current becomes bi-directional, which brings directionality issues to the protection scheme. Since distance protection is inherently directional, it solves this problem and secondly, distance is not affected by the changing fault current level due to changing source impedance compared with overcurrent protection.

3. Methodology

The chapter outlines the systematic approach deployed in this study to achieve objectives discussed in the introduction. As discussed, the purpose of this work is to model and simulate in real-time, a distribution system protection scheme with and without distributed generation. For a successful execution of the research work, a systematic method to achieve the final target was used.

3.1. Software selection

To accomplish the research work objectives, it is imperative that the chosen software has suitable features to allow modelling of the electricity distribution network, the renewable photovoltaic system and equivalent sources; it should also allow simulation of faults, hardware-in-loop (HIL) connection and perform relay coordination. The softwares under consideration that were checked for suitability were ETAP, PSCAD, RSCAD and Matlab.

Electrical Transient and Analysis Program (ETAP), by Operation Technology Incorporated, is power systems design, modelling, analysis and planning software that can be used for short circuit analysis, load flow study, transient study, user-defined dynamic model, modelling of PV arrays and protective devices coordination. Power System Computer Aided Design (PSCAD) is a time-domain simulation program predominantly dedicated to the study of transients in power systems. Its main function is the power system simulation in frequency and time domain. PSCAD can be used in power system and power electronic studies, harmonic research of AC systems, transient torque analysis as well as the HVDC system and commutation starting [58]. PSCAD also provides time domain graphical outputs.

RTDS is a parallel processing computation facility that incorporates both software and hardware for digital simulation of electromagnetic transient programs [59]. It encompasses two classes, being digital real-time simulation and hardware-in-loop (HIL) real-time simulation [60]. RSCAD, which is a user-friendly graphical user interface, further enables construction and power systems' analysis by the user. With a digital real-time simulation, the system modelled inside the simulator does not involve external interfacing whereas in the HIL simulation, certain parts of the digital simulation are replaced with actual physical components. RTDS comprises of accurate power system component models that represent complex elements used for creating physical power systems. RTDS is hence selected for the purpose of this research, due to its availability and suitable features for successful execution

of this work. Graphical results exported from the runtime module are plotted and displayed on Matlab. Following is a procedural and deeper insight into how the research was carried out.

3.2. Modelling of the distribution network in RSCAD

3.2.1. Draft programme

The electrical design of the distribution feeders is done by computing the various parameters of the network such as resistance, inductance and capacitance. Resistance plays an important role in determining losses since increasing the line current also increases the I^2R losses. The system model is then set up and parameters inserted in RSCAD/Draft, which enables the user to create a system in a user-friendly graphic interface [61]. It comprises of a three-phase AC supply input voltage with a 132 kV R.M.S. voltage at 60 Hz, which is further stepped down to 66 kV substation with each feeder further branching into several subsidiary 22 kV and 11 kV laterals that carry power close to the load points. In RSCAD library, all load model types are available and the constant active and reactive power dynamic load models are used as indicated in chapter 4.

All CT ratios corresponding to full load conditions are determined and set, voltages and currents at the transformers' primary and secondary windings of the transformers, the systems MVA ratings, base frequencies and source parameters are then checked and verified. The model is compiled, generating the executable code required by the RTDS to run the simulation. In case of any errors in the modelling stage, the compile process cannot be completed due to the possibility of unreasonable data for the network model and control elements, inconsistency as well as duplication of parameter and signal labels.

3.2.2. Runtime programme

After a successful compilation, the runtime module is then opened where available racks show with red indicators on the right side of the GUI environment. On runtime, different actions such as controls can be applied and their response observed and analysed by the aid of graphs and meters. A direct communication is enabled between the RTDS simulator and a PC with the modelled network. Firstly, the monitored variables and controlled elements are selected, which are then used for setting different events in the power-system model such as fault applications and switching. The compiled model is next loaded onto the simulator and

real-time simulation run. The system's power, voltage and current outputs are monitored and checked to see whether they produce desired results.

3.3. Protection set-up

Current transformers' appropriate choice and sizing is the first important phase in overcurrent protection settings [21] [62]. The selection of CT ratios is based on the system's full load current. Zones to be protected are then identified on the distribution system and for each zone overcurrent relays configured. The relays' pick-up currents are computed based on a chosen plug setting value and set. The characteristic curve selected for all relays was the IEC standard inverse curve.

Time dial setting (TDS) selection provides the necessary protection devices coordination [21] [63], and is dependent on factors such as the maximum fault current, selected IDMT curve type and the downstream circuit breakers' operating time. For the most downstream breaker, the TDS is set to a minimum value, simulations are then ran and coordination studies for all relays carried out systematically from downstream breakers up to the breaker closest to the source.

3.4. Protection relay testing

A hardware-in-loop connection was set up and verification of all software simulations results was accomplished by substituting the networks' software relays with the physical commercial relays. Current and voltage signals were exported from the RTDS using OMICRON CMC 156 amplifier and Gigabit-transceiver Front Panel Interface (GTFPI). Combination of the amplifier and the RTDS produces the actual conditions in which the relay will function during a fault.

3.5. PV generation system design

In order to simulate the behaviour of a solar panel, a fully functional photovoltaic array consisting of 150 modules in series and 300 modules in parallel was built and developed in RSCAD. For varying temperature and irradiation inputs, verification of all desired outputs from the PV model was carried out to understand the impact of the change in weather conditions. The PV array's operating point is maintained at the maximum power and output by using a fractional open circuit voltage based maximum power point trackers (MPPT). The tracker uses the fact that the PV array voltage corresponding to the maximum power displays

a linear dependence relating to array open circuit voltage for varying temperature and irradiance.

3.6. Grid-tied inverter model development

For a grid-tied photovoltaic generation system, three-phase inverters are used to convert the DC output into a three-phase AC power [64]. A photovoltaic inverter was configured and coupled with the distribution network. The essential interface to bridge the large and small time-step simulation portions is created by transferring voltage and current information between them. Voltage information from the large time-step side of the simulation is transferred to the small time-step side and current information from the small time-step side is brought to the large time step side. Using this interface technique allowed the necessary power electronics application device to be accurately modelled and simulated with the PV array model. The main network is then connected to the small time-step sub-network through three single-phase interface transformers.

3.7. Stand-alone grid tied PV system

The inverter was connected to transformers' low voltage side and the high voltage to the grid represented by a constant 11 *kV* voltage source. The PV generation system was then connected to the utility network using the 11 *kV* busbar as the point of common coupling. Steady state results and performance outputs of the whole distribution network and PV inverter system were then monitored and verified. The PV system fault current contribution impacts on the capacity of protection components in the distribution network was investigated and using dual simplex method, relay coordination was achieved. A study was done on the modelled system to support the theoretical expectations regarding possible outcomes. The point of common coupling was changed to the 66 *kV* busbar to determine PV penetration impacts on different sections of the network.

3.8. Optimal relay coordination

Tap settings such as the current and time dial setting must be determined for relay coordination. Full load and minimum fault currents assist in determining all relays' current settings [3] [65]. For the time multiplier determination of all the overcurrent relays protecting the distribution system, the sum of all relays' operating times are optimized using an optimization technique [65]. Techniques under consideration were generic algorithm, partial

differentiation approach, particle swarm optimization and dual simplex method, of which the dual simplex method was selected.

The regular simplex method was modified and developed by Lemke into dual simplex method to solve linear programming problems (LPP). The technique results in the solution to becoming feasible and optimal at some stage through an iterative computation [65]. Assuming that the OC relay's TMS and plug setting are specified, its time of operation can be calculated for a known fault current using the following mathematical equation (5) above. Below is the algorithm of the dual simplex method used to solve the maximization problem [65] [66].

- a) Start.
- b) Convert the problem into maximization problem.
- c) Convert all the constraints into \leq type.
- d) Rewrite the functions into standard form by adding surplus variable, which are basic variables.
- e) Form the Dual Simplex table.
- f) Find $C_j - \sum(C_j * a_{ij})$
 - If any $C_j - \sum(C_j * a_{ij})$ element becomes non-negative, go to step (j).
 - If all the elements in this row become non-positive and if all the elements in the RHS column are non-negative, go to step (i).
 - If at least one element in RHS is negative, go to step (g).
- g) Form a dual simplex table after identifying the key column, key row and pivot element.
- h) Go to step (f).
- i) Print results
- j) Stop.

3.9. PV impacts mitigation methods

When high PV penetration levels, the grid is subjected to several negative impacts hence the grid flexibility requirements need to increase. The status of and major obstacles to the establishment of DG within utility systems was then presented and potential solutions discussed. Implementations have been made to address the issue of reviewing present protection settings for a reliable protection coordination establishment. Protection method

against islanding was implemented to provide basic detection of faults that will separate the DG from the utility during an islanded mode [67] [68].

3.10. Recommendation for future works

Fields of future investigation were identified and described at the end of the research work. As mentioned in the literature, distributed generation will be a trend in the near future hence there will be a high volume distributed generations in the distribution systems. The implemented anti-islanding technique is not an optimal choice for high-density PV systems and will have some limitations in future; therefore, the work was carried out to enable the use of its outcomes for further build up and refining for future research.

4. Modelling and real-time simulation

4.1. Test distribution system configuration

Real-time protective relaying is an effective and widely used technique that has been used for decades by power distribution utilities for protection [31]. The real-time simulator employed in this work is the RTDS simulator by RTDS technologies. The RSCAD is a graphical user interface with wide model libraries permitting an extensive range of electrical system architectures and components designs. Shown in Figure 1 is the modified test distribution system's single line and block diagram in which the proposed overcurrent protection method is tested. For purposes of this research, a radial line configuration was considered because it is the most commonly encountered distribution network configuration and ideal for illustrating the time overcurrent protection scheme [31], with the full model shown in the appendix Figure 42. The input voltage is a three-phase AC supply with an R.M.S. voltage of 132 kV at 60 Hz, which is further stepped down to 66 kV. Each feeder which emanates from the 66 kV substation branches further into several subsidiary 11 kV and 22 kV feeders to carry power close to the load points where a transformer further reduces the voltage from 11 kV to 380 V for customers.

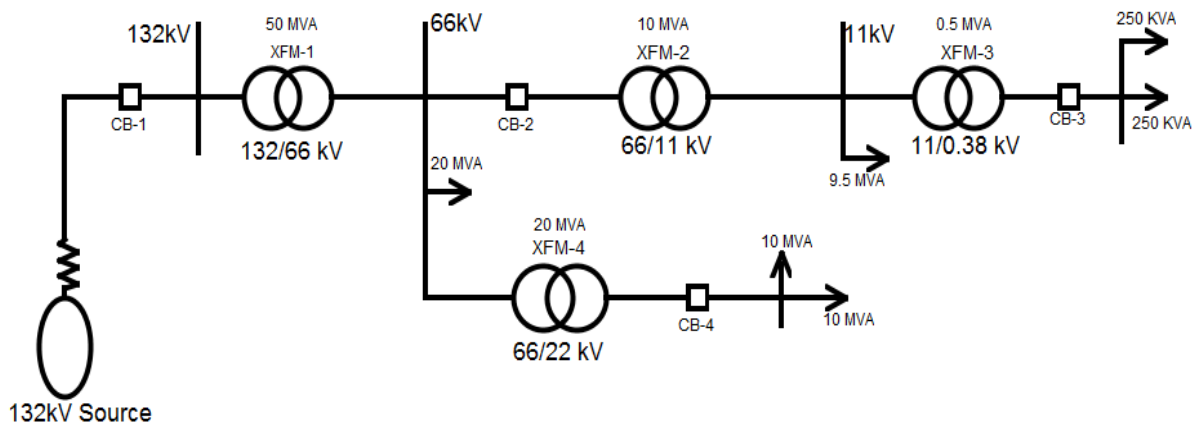


Figure 1: Single line diagram of the modelled distribution system

Current transformers' appropriate choice and sizing is the first important phase in overcurrent protection settings [62]. The CT ratios and overcurrent relays are configured for each protection zone. The network comprises of four main protection zones denoted by circuit breakers labelled CB-1, CB-2, CB-3 and CB-4, of which the corresponding protection equipment should be set up to ensure adequate protection coordination. The system comprises of diverse consumer characteristics, ranging from high consumption households during holidays, to those that are more active at night, the industrial consumers working 8-

hour shift and those who constantly work. Because of the diversity of consumers, the distribution system is loaded diversely on a daily, monthly and annual basis. Table 1 presents the loads and the system parameters.

Table 1: Transformers, load and source parameters

<i>Transformer</i>	<i>Ratio</i>	<i>MVA</i>	<i>Load Data</i>			
XFM-1	132/66 kV	50	<i>Load</i>	<i>P (MW)</i>	<i>Q (MVAR)</i>	<i>S (MVA)</i>
XFM-2	66/11 kV	10	1	18.5	7.5	20
XFM-3	11/0.38 kV	0.5	2	9	4	10
XFM-4	66/22 kV	20	3	0.23	0.09	0.25
<i>Voltage Source Parameters</i>			4	0.23	0.09	0.25
MVA	120	5	9	4	10	
Frequency	50 Hz	6	9	4	10	
Voltage	132 kV					

In the radial distribution system shown, there is only one path, which connects end-users with the source. This path is one-way, hence there is a unidirectional flow of current from the source, which means only the source provides electric power to end-users. If there is a power outage, the end-users lose electric power completely. Protective relays identify unwanted conditions within the network, and then trip the circuit breakers to isolate the faulted area before any damage or interference with the operation of the distribution network as a whole [69].

4.2. System full load conditions

The section concisely presents findings and results obtained from simulations of the modelled distribution system. To begin with, all model equipment parameters are set and the system is run on RSCAD. Shown in Table 2 are bus voltages, line voltages and currents as seen from the power and current transformers for input to the overcurrent relays.

Table 2: Voltages and Currents measured on the distribution system.

<i>Parameter Voltage</i>	<i>Value</i>	<i>VT secondary Voltage</i>	<i>Parameter Current</i>	<i>Value</i>	<i>CT Secondary Current</i>
<i>Bus-1</i>	132 kV	109.8 V	<i>IB-1</i>	0.185 kA	1.088 A
<i>Bus-2</i>	10.98 kV	109.7 V	<i>IB-2</i>	0.091 kA	0.8741 A
<i>Bus-3</i>	0.379 kV	109.3 V	<i>IB-3</i>	0.752 kA	0.752 A
<i>Bus-4</i>	21.89 kV	108.9 V	<i>IB-4</i>	0.304 kA	1.042 A
<i>Bus-5</i>	65.96 kV				

In the no fault scenario, normal RMS currents flow through the CTs and there is no disturbance in the currents. The current pick-up value for a breaker to generate a trip signal should be at least 1.2 times of the normal full load RMS current [70]. The current setting is selected to be above the maximum short time rated current of the circuit involved and since all relays have hysteresis in their current settings, the setting must be sufficiently high to allow the relay to reset when the rated current of the circuit is being carried.

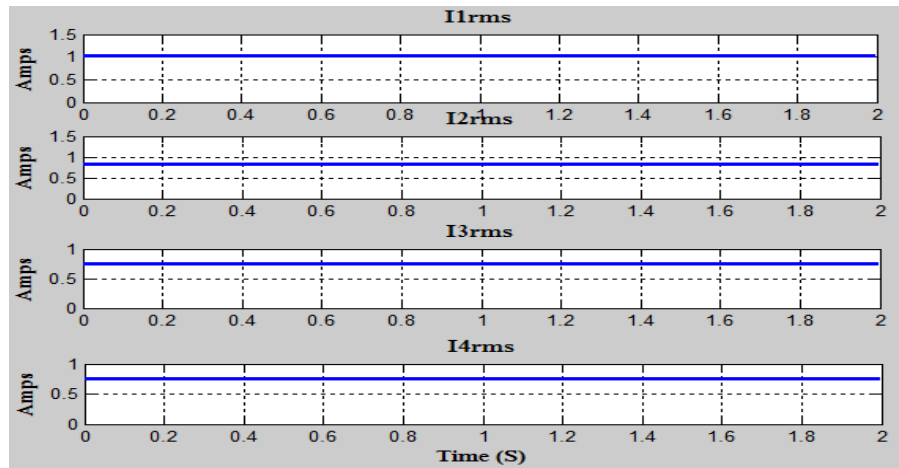


Figure 2: System R.M.S Currents

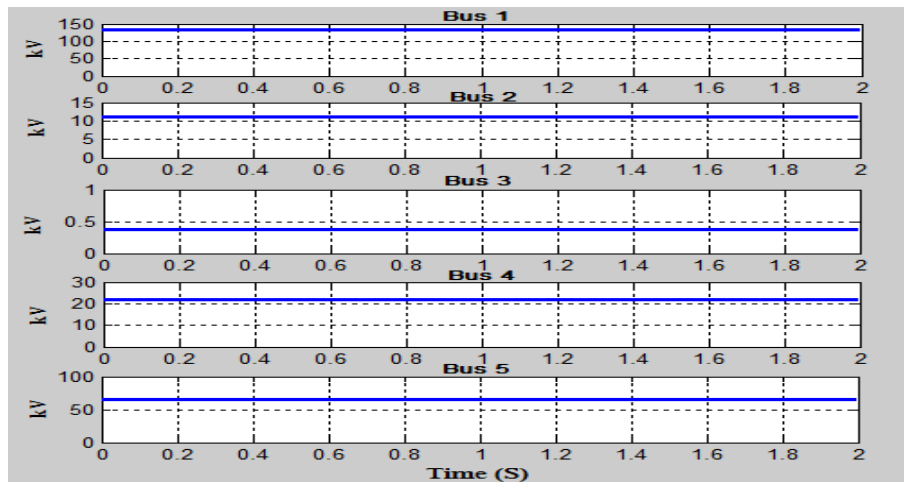


Figure 3: Distribution system RMS voltages

Shown in Figure 2 and Figure 3 are full load current and bus voltages of the distribution system modelled at no fault. Figure 2 shows the system RMS currents as seen from the CTs secondary windings. It can be seen that at no fault operating conditions, there is a constant current flowing from the source to the dynamic loads in the different radial system laterals. The voltage levels read are as initially set for the system design in section 4.1, with a small deviation due to the system impedance and loads' reactive power.

4.2.1. Fault and breaker logic control

To verify the fault levels in the system to different branches of the network, faults are applied on the distribution feeders. For convenience, ability to control the fault type, fault location and closing of the circuit breakers during runtime is necessary. Shown in Figure 4 is the fault logic which enables fault application and changing in the runtime interface. The logic is advantageous in provision of a more efficient way of testing as opposed to switching between the draft and runtime interface to implement changes to the faults on the system. It allows activation of fault using a push button, selection of and alteration between the different combinations of line to ground faults via a dial switch as presented in Table 7 that shows the binary and dialing outputs along with the corresponding fault type.

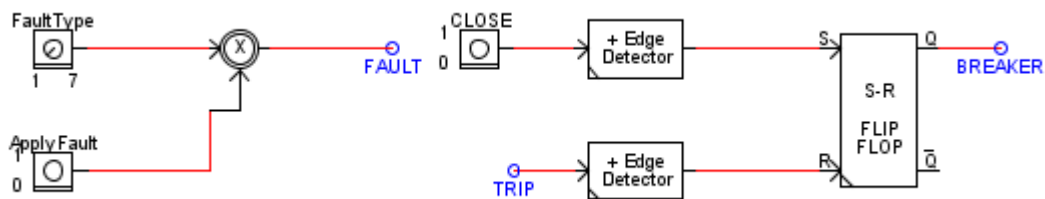


Figure 4: Fault and circuit breaker logic

For the design, all the three phases in the distribution lines of the system have to be protected even if a fault occurs on either single line, double lines or all the three phases. A single logic input is used to open and close the circuit breaker model in the simulator. The circuit breaker model is designed to respond to separate open and close commands by means of an SR flip-flop component. In the system, once the relay issues a trip command to the breaker logic shown in Figure 4, the circuit breaker receives the signal to open; which can be closed by means of a ‘close’ push button in runtime.

4.2.2. Relay logic control

The time overcurrent relay forms the vital fragment of the protection scheme, hence its functionality takes up a significant role in operating as a decision making component in the protection scheme. For operation, the relay is activated by the voltage and current transformers’ voltage and currents measurements respectively. If an abnormal condition exists, the relay then decides if it is large enough to endanger the system followed by an appropriate preventative action to protect the system. Shown in Figure 5 is the multi-functional overcurrent relay that is suitable for providing the protection function on distribution system lines with the (51/67P) overcurrent element (PTOC) enabled. The

secondary phase voltages and currents are fed into the six inputs of the relay. These voltage and current phases are from the secondary side of the voltage transformer and current transformer respectively. The RMS quantities are calculated and a comparator functions to determine whether the magnitude of the measured current is greater than the set point value. If any phase current or residual current is greater than the set point value the comparator output causes the start and info signals to become active then the trip signal becomes active after some time delay.

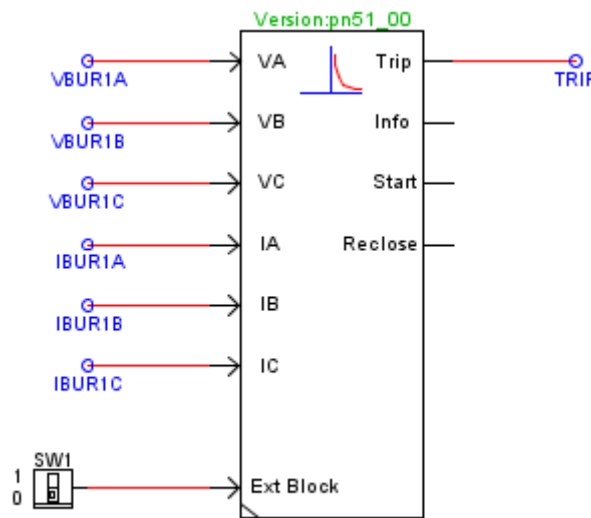


Figure 5: Software overcurrent relay used

The external block serves as a user controller to lock or unlock the relay which is necessary for relay maloperation simulation.

4.3. Software relays' simulation:

4.3.1. Testing software Relay-3

This section replicates the system in RSCAD where the manifestation of faults on the distribution system is closely observed for various faults location and types. The downstream circuit breaker CB-3 is set to function under the control of relay-3, which enables the breaker to open the circuit when required. It is also necessary that relay-3 be coordinated with upstream relay-2 for desired system protection discrimination. Inverse time relays are adjusted by selecting time dial and current settings.

On setting up the protection system, relay-3 current setting of 1.25 is chosen and the time dial setting set to minimum for the fastest possible fault clearing time, enabling CB-3 to clear the

high current fault in a very short time. From Figure 2, it can be seen that the RMS current is found to be 0.752 A, giving a pick-up current of 0.940 A.

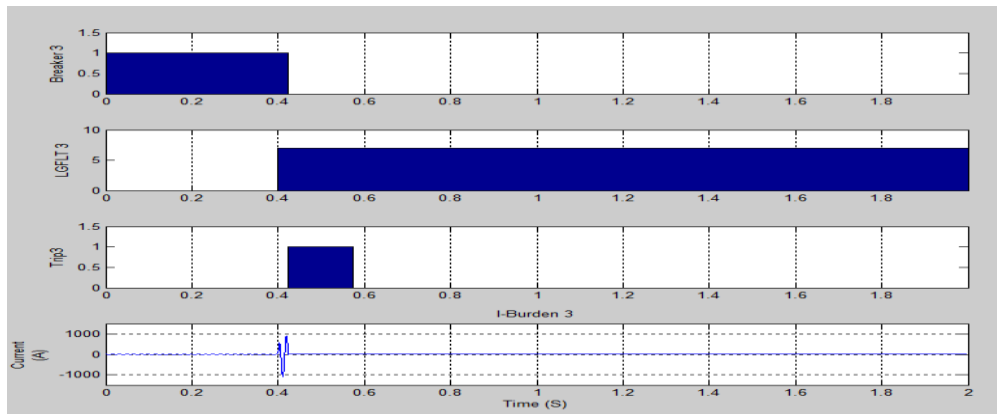


Figure 6: Relay-3 operating for a fault on 380 V busbar

Figure 6 shows the analysis of events that take place when a fault on the 380 V busbar is applied. A fault is applied at 0.4 *seconds*, the fault current rises and is seen across the current transformers as 1096 Amps due to 1000:1 CT ratio. Owing to a trip signal received from relay-3, the CB-3 opens, clearing the hazard from the system. Taking the time multiplier setting for the relay to be the minimum 0.025, the time of operation is calculated theoretically as 0.0230 *seconds* for the relay. From the software simulation, the circuit breaker opens at 0.4233 *seconds*, giving a time of operation of 0.0229 *seconds*, hence it can be concluded that the theoretical calculated time of operation is approximately equal to the time of operation obtained from the graph.

With protective relays, the goal is to allow enough time for the relay and breaker closest to the fault to clear the fault from the system before the backup relay associated with the adjacent section to the source opens its circuit breaker. The time interval allowed between two adjacent relays' operation in order to achieve correct discrimination between them is called the grading margin. Taking into consideration factors such as circuit breaker operating time, relay overshoot time, contact gap together with relay and CTs errors, a time grading margin of 400 *ms* is used, as recited from the MiCOM relay user manual.

4.3.2. Time setting of Relay-2:

Relay-3 and relay-2 coordination is achieved by evaluating the maximum fault current seen by relay-2 for a fault at protection zone-3, denoted by circuit breaker CB-3. On adding a 0.4 *seconds* grading margin, the time of operation for relay-2 on failure of relay-3 will be 0.4231 *seconds*.

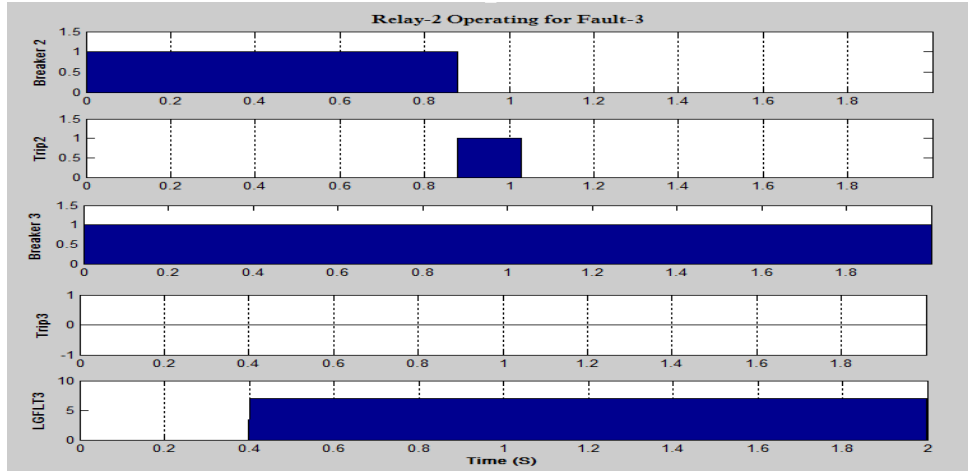


Figure 7: Relay-2 testing for a fault at zone-3 (380V busbar)

Figure 7 shows the expected outcome of relay-2 time of operation for a fault at zone-3, which is found to be *0.4269 seconds*. To determine the time dial setting for relay-2, fault-3 current is transposed onto the 66 kV line and calculated to be *6310 Amps*. Taking the time of operation calculated above, the multiplier setting is calculated as 0.25.

4.3.3. Testing software Relay-2:

Using a 0.25 multiplier setting on relay-2, a fault is applied and the time of operation then verified with the runtime graphs. With a fault current of *1.04 kA* on the 11 kV bus, the time of operation is calculated to be *0.2395 seconds* while Figure 8 gives the time of operation of *0.0244 seconds*.

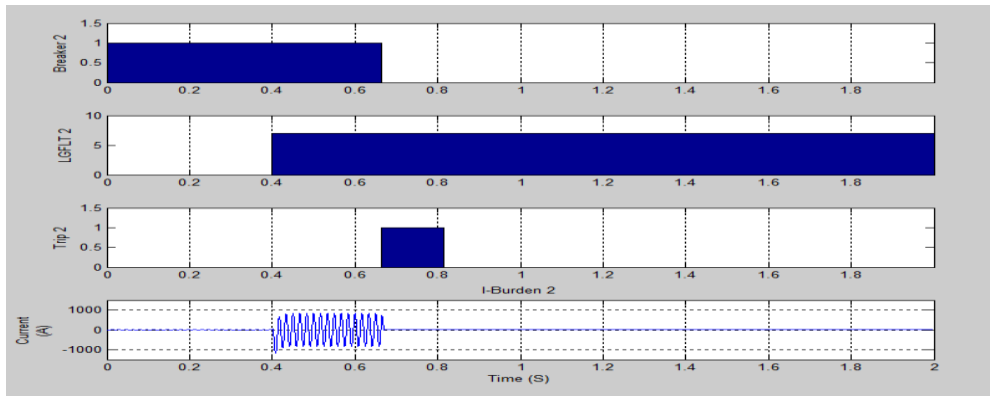


Figure 8: Relay-2 operating for a fault at zone-2 (11 kV busbar)

For relay-2, the pick-up current is calculated to be *1.14 A*. The *626 kA* fault current is seen from the CT secondary windings as *1.04 kA* due to the transformer XFM-2 and 100:1 CT ratio. Taking the TMS calculated above, the computed time of operation is *0.2395 seconds* which is equivalent to *0.2538 seconds* obtain from Figure 8 simulation results.

4.3.4. Time setting of Relay-1:

From Figure 9, relay-1 time of operation for fault-2 is found to be 0.7197 *seconds*. As expected, breaker-1 opens at 1.120 *seconds*, which is approximately 0.4 *seconds* later than the time breaker-2 should have opened, confirming proper relay coordination on the distribution system.

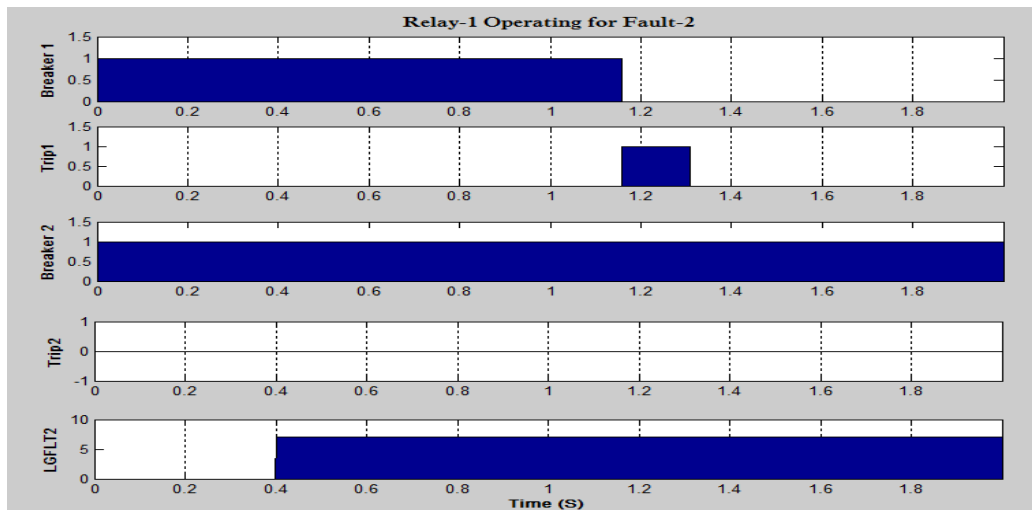


Figure 9: Relay-1 operating for a fault at zone-2 (11 kV busbar)

As seen, Figure 9 confirms and verifies the expected outcome of relay-1 time of operation for a fault at zone-2. As carried out previously, relay-1 time multiplier setting is calculated and set up so it operates for a fault at protection zone-2. Following are calculations carried out in determining the time dial setting for relay-1. Fault-2 current transposed onto the 132 kV line is calculated to be 52.17 kA and is seen across the relay coils as 260 A due to 200:1 CT ratio. Taking the time of operation calculated above using margin grading, the time multiplier setting for relay-1 is calculated to be 0.52 and therefore set to 0.55.

4.3.5. Testing software Relay-1:

With all relay-1 parameters and time multiplier setting determined and set, fault-1 is applied and the time of operation calculated and verified with the runtime graphs. Figure 2 shows a 132 kV distribution line full load RMS CT secondary current of 1.088 *Amps*; hence, relay-1 pick-up current value is calculated to be 1.36 *Amps*. A 26 kA fault current is seen in the relay coils as 130 *Amps* due to the CT ratio. Taking the time multiplier setting for relay-1 as 0.55 calculated above, the time of operation is 0.7780 *seconds*.

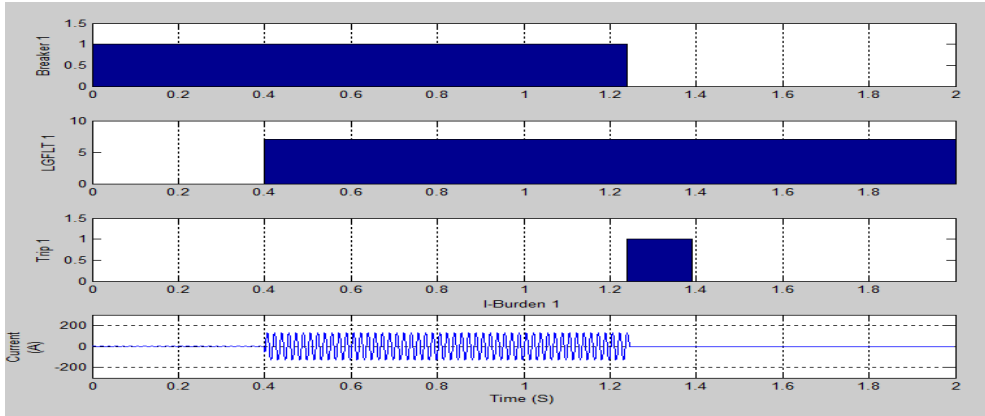


Figure 10: Relay-1 operating for a fault at zone-1(132 kV busbar)

The time of operation of the relay-1 is calculated to be 0.7997 s from Figure 10. This confirms the time of operation for the relay, which is equivalent to the manually calculated value 0.7780 *seconds*.

4.3.6. Testing software Relay-4

Relay-4 is downstream on the 22 kV distribution system lateral and is tested for a fault occurring at protection zone-4. The time multiplier setting for the relay is also set to a possible minimum and the manual calculation of the time operation carried out and verified. Relay-4 pick-up current is set to 0.9511 *Amps*. Using the minimum 0.025 time multiplier setting for relay-4, the time of operation is calculated to be 0.03 *seconds*.

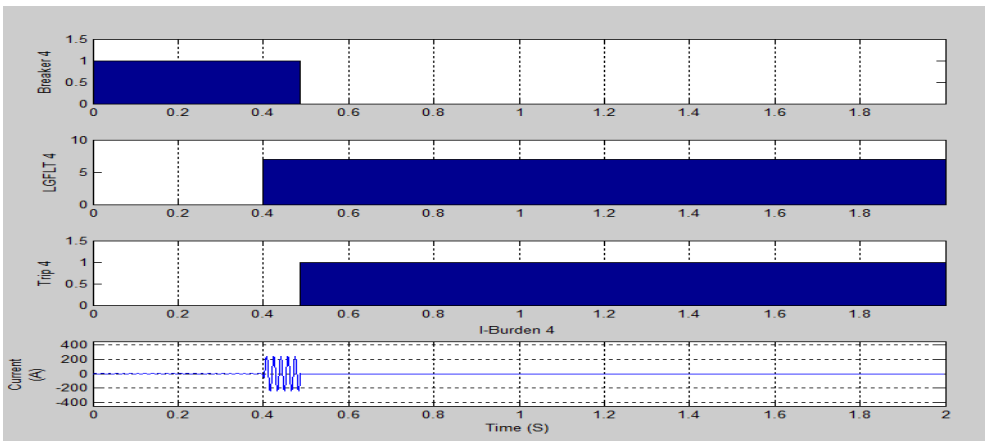


Figure 11: Relay-4 operating for a fault on the 22 kV busbar

As observed in Figure 11, the time of operation obtained experimentally, 0.0330 *seconds*, confirms the previously calculated relay-4 time of operation of 0.03 *seconds*.

4.4. Protection Coordination results

Overcurrent protection scheme is implemented for coordination of relay of interest with upstream relays, which refers to the supply side or higher voltage side of the system. For a radial network, the coordination is done for the feeder protection with upstream protection. If the first and second breakers from the fault zone both fail to operate, the circuit breaker closer to the source should open [70]. Therefore, for a fault on bus 3, relay-3 is set to operate faster than relay-2 by a time-delayed approach thus defining primary and backup protection zones. The design approach is mentioned in the previous sections.

Figure 12 and Figure 13 display simulation results showing proper relay coordination for the distribution system under study. To simulate the proceedings of events that occur in case of a failure to send or receive the trip signal resulting in a failure of the relay, relays of interest are disabled by deactivating the trip signal that governs the breaker so it does not open for a fault on the protection zone. Following is the simulation of relay-2 malfunction; the trip signal governing the 66 kV breaker is deactivated, disabling it to open for a fault on the line. Simulation studies are done by applying a fault and observing the upstream active relay's response.

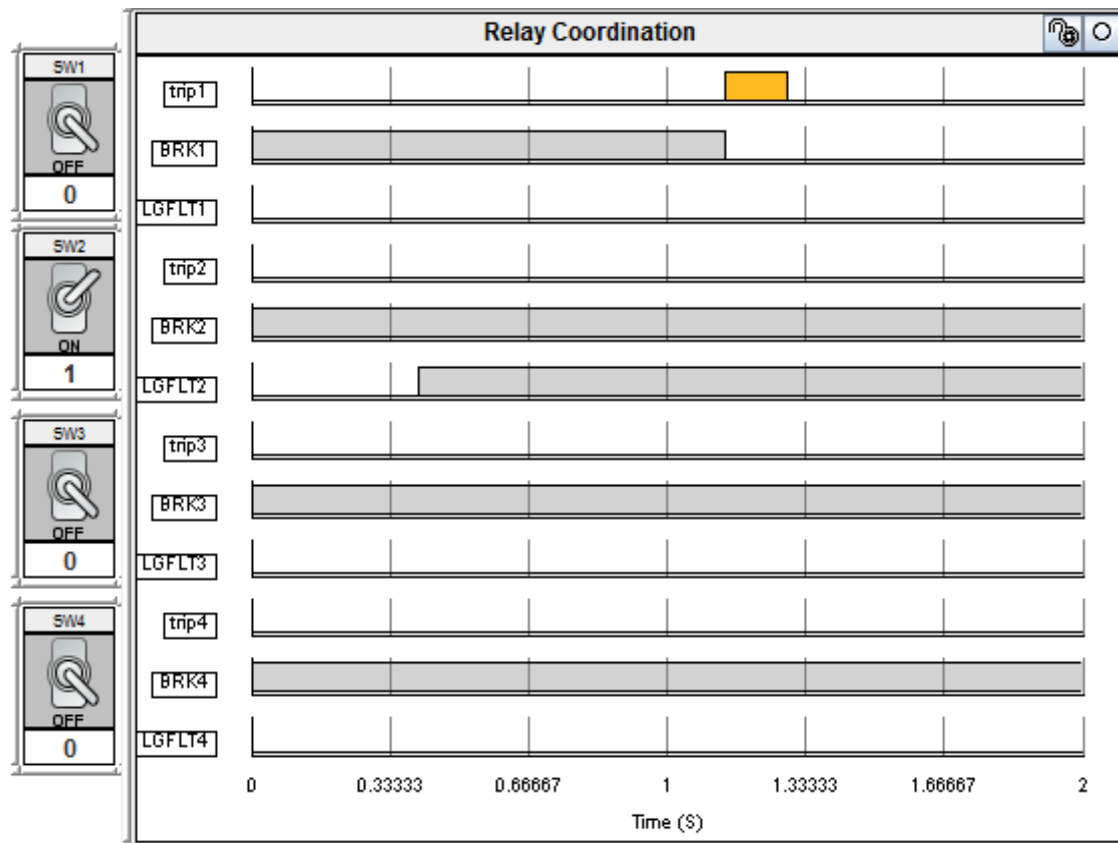


Figure 12: Relay-2 failing to operate

From Figure 12, verification of the 132 kV upstream breaker is done, which opens as a response to a fault occurring at zone-2. As expected, breaker 1 opens at 1.15 seconds, which is approximately 0.4 seconds later than the time breaker-2 should have opened. Since the circuit breaker closest to the source opens, there is no current flow to other parts of the distribution system.

4.4.1. Testing coordination of relays 3, 2 and 1

In this section, relay-3 and relay-2 are disabled to verify coordination between them. A fault is applied at zone-3, followed by observations as to whether the fault is cleared by the upstream breaker closest to the source. Shown in Figure 13 are the graphs obtained when relay-3 and relay-2 fail to operate.

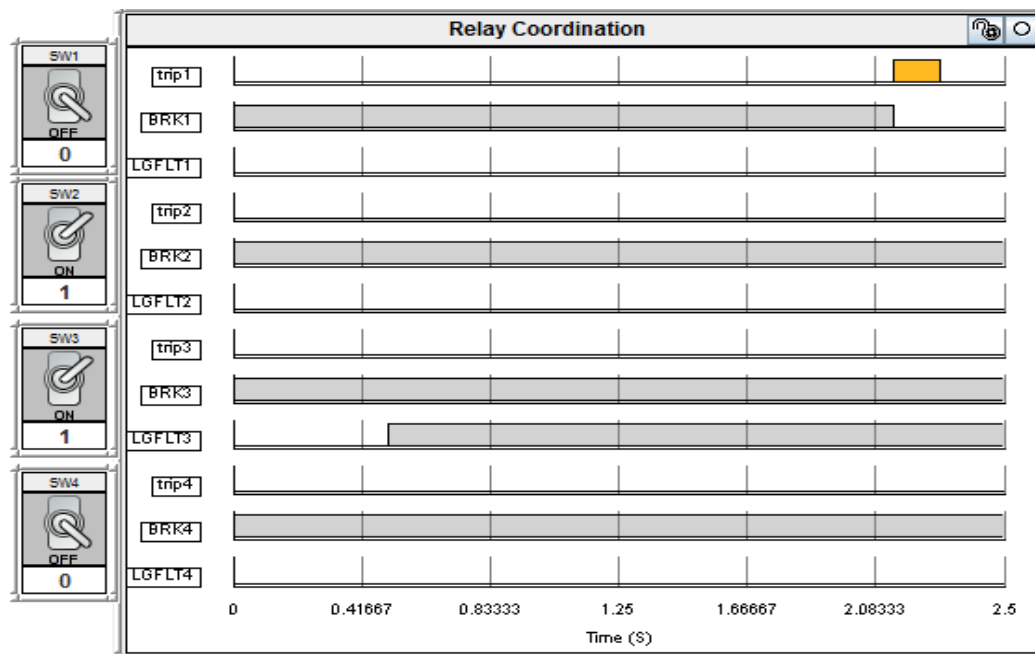


Figure 13: Failure of relay-3 and relay-2 to operate

As can be deduced from Figure 13, the fault on the 0.380 kV busbar was activated at 0.50 seconds. The 132 kV breaker opens at 2.235 seconds since the 66 kV breaker failed to open, giving 1.735 seconds as the time of operation. This is as desired since distribution system philosophy is that the upstream breaker will open slower than the 66 kV and 0.38 kV downstream breakers.

4.4.2. Testing coordination of relays 3 and 2

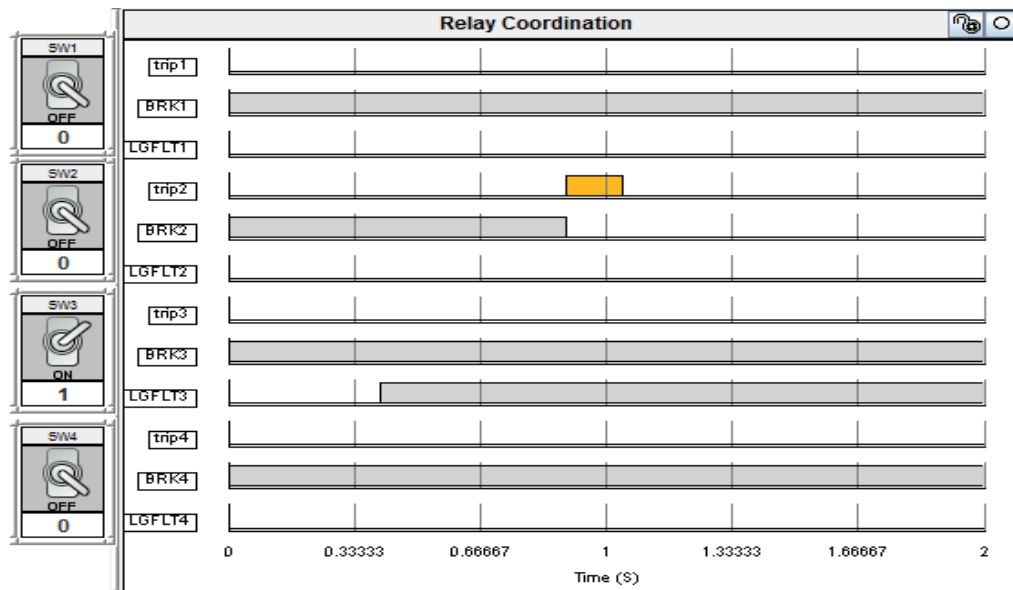


Figure 14: Operation of relay-2 for a fault at protection zone 3

Using 0.4 seconds grading margin, the time of operation for relay-2 on failure of relay-3 to operate is calculated to be 0.4231 seconds. Calculated from Figure 14, the time of operation of the relay is 0.4269 seconds. The simulations results show that the time of operation for relay-2 is approximately equal to the manually calculated one, which goes in agreement with theory that relay-2 will operate 0.4 seconds later than relay-3 would have operated.

4.4.3. Testing coordination of relays 4 and 1

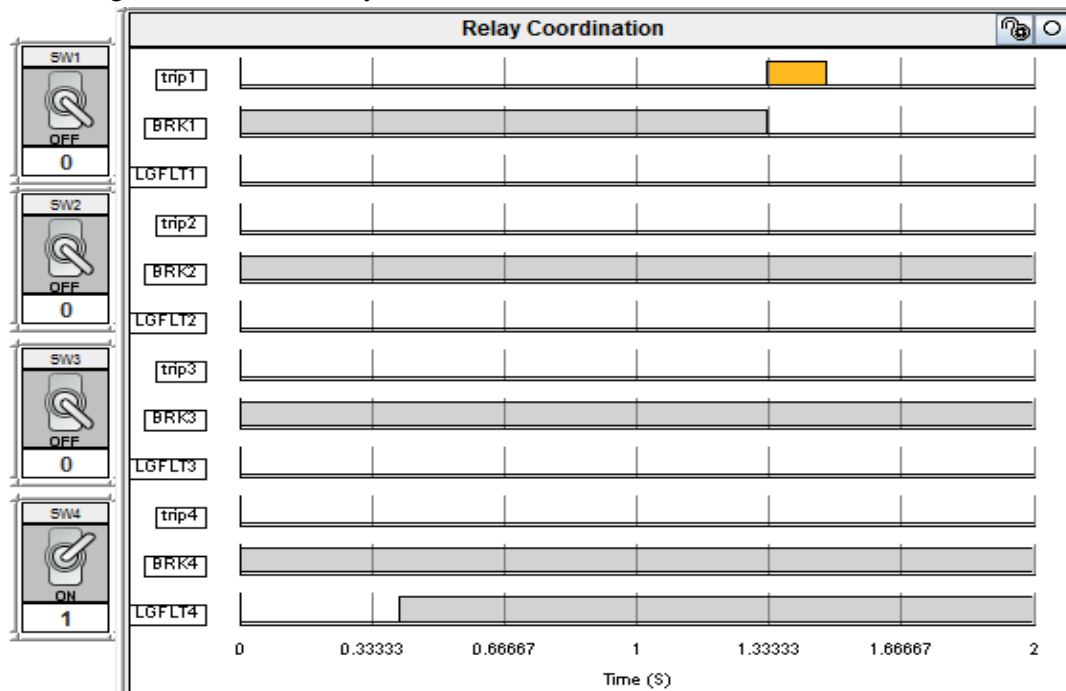


Figure 15: Relay-4 failing to operate

As seen in Figure 15, the graphs depict results pertaining to relay-4 failure, which is disabled and a fault applied at protection zone-4. The relay responds in 0.9499 *seconds* by sending a trip signal to open the upstream circuit breaker and clear the fault, thus confirming coordination between relay-1 and relay-4.

5. Experimentation and Verification

5.1. Hardware-in-loop simulation

Verification of all results obtained from the software simulations is achieved by substituting the software relays on the network with the hardware relays. This section considers the performance of hardware relays in a hardware-in-loop connection with the software distribution model. As depicted in the appendix Figure 43, Gigabit-transceiver analogue output (GTAO) and GPC processor cards are configured in RSCAD for the connection between the RTDS simulator, external protection and control devices replacing the software components. For exportation of the current signals from the RTDS, OMICRON CMC 156 amplifier and Gigabit-transceiver Front Panel Interface (GTFPI) are used. During a fault, the relay generates a trip signal which is sent back via GTFPI to the RTDS, which causes disconnection of a corresponding circuit-breaker in the distribution network model.

The relay input is connected to the RTDS analogue/digital output which is connected to the power amplifier as shown in Figure 16. The analogue/digital output of the relay is then connected with the analogue digital input of RTDS. The signal level analogue output voltages sent from the rack in real-time are converted to correctly-scaled currents and voltages for input to amplifier. In this way, the real time simulation can be used to drive the relay with the same power level currents and voltages it would experience in the field [71]. From the amplifier, these currents are fed to the relay which produces a trip signal when tripping conditions are fulfilled.

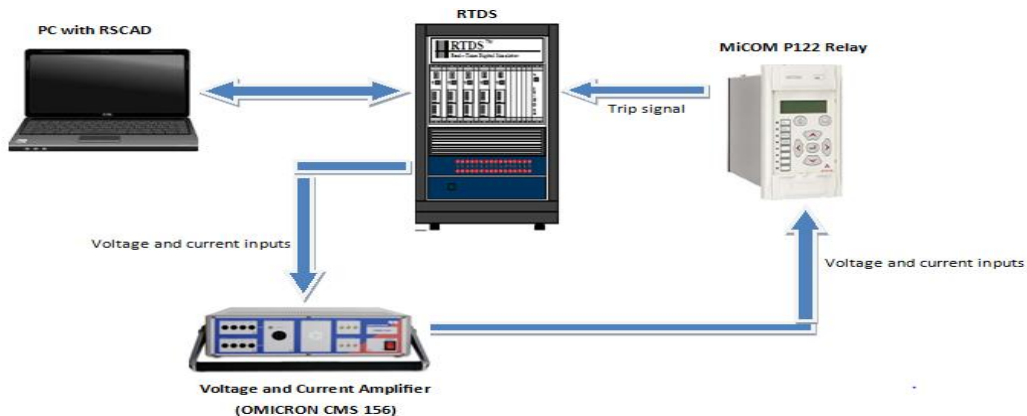


Figure 16: System hardware-in-loop connection

The relay receives current and voltage signals from the secondary side of instrument transformers of the system simulated on the host PC through digital to analogue conversion

and necessary amplification stages. One at a time, the software relays are replaced with the MiCOM P122 and simulations run to verify results obtained while using the software relays. Figure 17 to Figure 20 show hardware relays 1 to 4 operating in the distribution system through a hardware-in-loop connection and same settings used for software relays are in the similar manner are set for the hardware relays.

5.1.1. Testing Hardware Relay-3

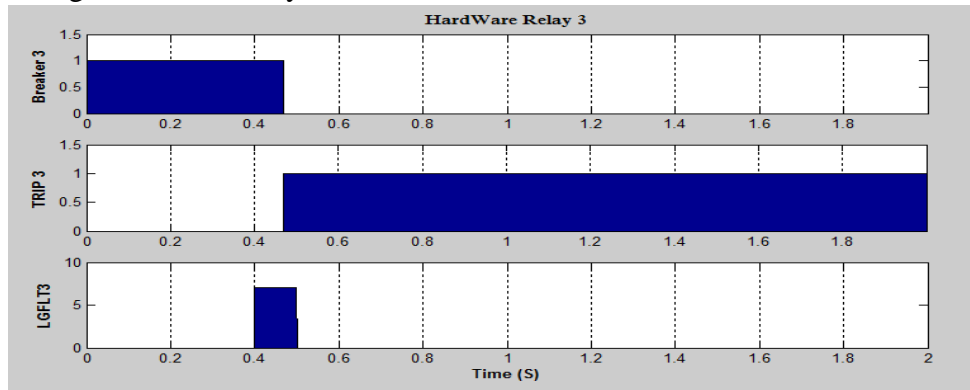


Figure 17: Hardware Overcurrent Relay 3 operating

5.1.2. Testing Hardware Relay-2

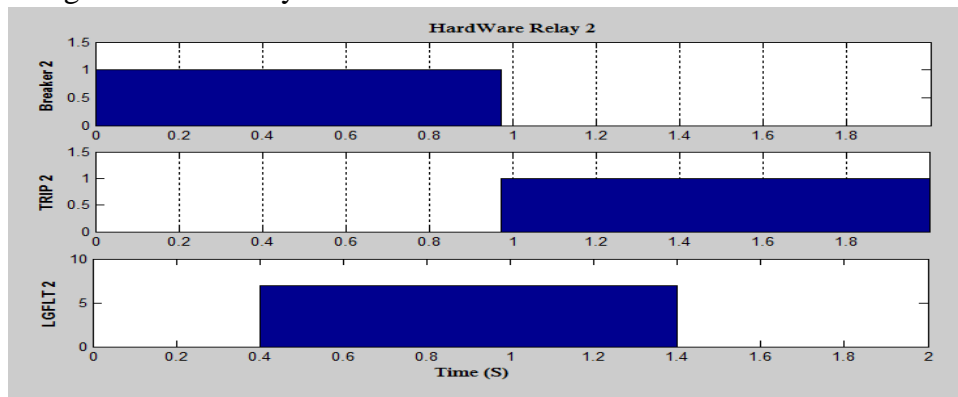


Figure 18: Hardware Overcurrent Relay 2 operating

5.1.3. Testing Hardware Relay-1

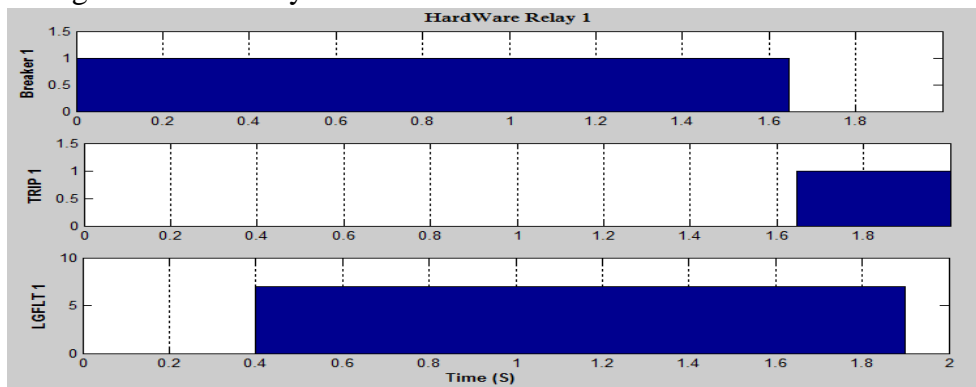


Figure 19: Hardware Overcurrent Relay 1 operating

5.1.4. Testing Hardware Relay-4

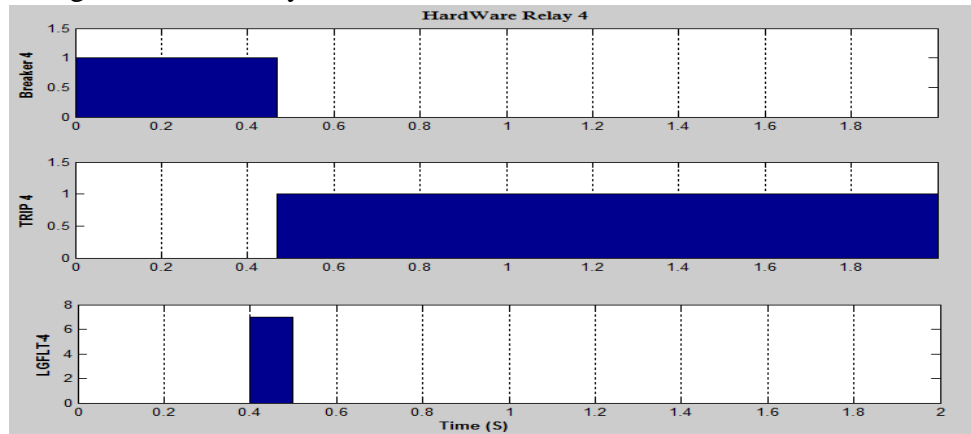


Figure 20: Hardware Overcurrent Relay 4 operating

A comparative study for protection coordination of overcurrent relays is presented for different configurations using both software and hardware relays. From above figures, a conclusion that verification using hardware relays was accomplished can be drawn. All the relays were tested for line-line and 3-phase to ground faults.

Table 3: Comparison of operating time from software and hardware relays

Relays	Theoretical value	Software relay	Hardware relay	% Difference
Relay 1	0.778 s	0.7990 s	0.821 s	2.69
Relay 2	0.2395 s	0.2438 s	0.273 s	1.79
Relay 3	0.0230 s	0.0229 s	0.035 s	0.44
Relay 4	0.0321 s	0.0330 s	0.038 s	2.80

Shown in Table 3 is the relays' time of operation obtained from the software and hardware simulations. The results are compared with the theoretical values obtained from manual calculations which as expected are approximately equal, with percentage deviations below 3%. As seen in the results, there is a relatively higher time of operation for hardware as compared to using software relays. The discrepancies in the time of response of the relays are influenced by the adjusted time multiplier setting when using hardware relays since they are standard setting so values could not be used exactly as manually calculated and the possibility of delays from the voltage and current amplification stage. It was also due to the fact that during the hardware simulations, settings were modified slightly with regards to increasing fault duration on the distribution system while using hardware relays to allow sufficient time to pick up.

5.2. Grid-connected PV system

A complete RSCAD simulation of the grid connected PV system with the MPPT algorithm, power active and reactive control of the grid-side inverter has been carried out with the following parameters tabulated in Table 4. The system is composed of 255 W PV modules, Maximum Power Point Tracking (MPPT) modified fractional open circuit voltage tracker, the full bridge inverter circuit with filter and step-up transformer, synchronizing system and the connected load. Grid inverter is the core part of PV system connected to the grid. It has the same grid frequency and its power factor is approximately close to unity.

Table 4: Parameters of Mitsubishi Electric Photovoltaic Module

Parameter	Value
STC	$1000 \text{ W/m}^2, 25^\circ \text{C}$
Maximum power rating P_{max}	255 W
Short-circuit current I_{sc}	8.89 A
Open-circuit voltage V_{oc}	37.8 V
Maximum power voltage V_{mp}	31.2 V
Maximum power current I_{mp}	8.18 A
Normal operating cell temperature	45.7°C
Temperature coefficient	
I_{sc}	$0.056 \% / ^\circ \text{C}$
V_{oc}	$-0.350 \% / ^\circ \text{C}$
P_{max}	$-0.450 \% / ^\circ \text{C}$

A PV module with the specifications outlined in Table 4 is used. 150 series connected modules and 300 parallel-connected modules are used to form the PV array. As shown in Table 5, for the reference solar intensity of 1000 W/m^2 and 25°C , the expected PV array output voltage and power at STC will be $37.8 \text{ V} \times 150 = 5.67 \text{ kV}$, and $255 \text{ W} \times 45000 = 11.47 \text{ MW}$ respectively.

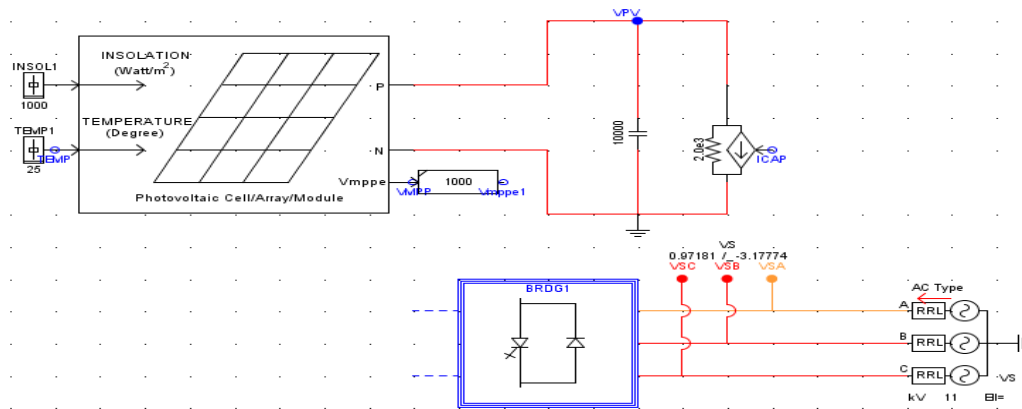


Figure 21: RSCAD model of grid connected PV system

A typical grid connected PV system is considered for simulation to study the impacts of connecting PV to the grid. The configuration of the PV model simulated for purposes of this study is shown in Figure 21. The network consists of a 10.2 MW PV generation system, which is integrated to the grid by means of a DC/AC inverter, a step-up transformer and the 11 kV bus as the point of common coupling. The inverter, presented in the appendix Figure 46, forms the core of the grid connected PV system and is responsible for the quality of power injected into the grid.

As stated in the literature, the solar I-V characteristic is highly nonlinear and changes with irradiation and temperature. In general, there is a unique point on the I-V curve called the maximum power point (MPP) at which the PV array operates at maximum efficiency [72]. Maximum power point trackers (MPPT) are used to maintain the PV array's operating point at the MPP to maximize its output. In this work, a fractional open circuit voltage based MPPT for photovoltaic array is used. The fractional open circuit voltage based MPPT utilizes the fact that the PV array voltage corresponding to the maximum power exhibits a linear dependence with respect to array open circuit voltage for different irradiation and temperature levels. The minor setback for this method is the power loss since the PV array is disconnected from the load after regular intervals for the sampling of the array voltage.

5.2.1. Inverter model development

Grid connected PV generator systems always utilise a connection to the electrical network via a suitable inverter because a PV module delivers only DC power. The RTDS is capable of simulating sub-networks containing IGBTs and other devices modelled as ideal switches, which is generally referred to as voltage source converter (VSC). Each VSC circuit is solved as a sub-network and can be interfaced to the main network solution, which is solved with a normal time-step size of 50 μ s whereas the VSC circuit is solved with a time-step of 1.4 to 2.5 μ s. The essential interface to bridge the large and small time-step portions of the simulation is created by transferring voltage and current information between them. Voltage information from the large time-step side of the simulation is transferred to the small time-step side and current information from the small time-step side is brought to the large time step side. The node voltage in the large time step side is transferred to the small time-step side, driving a voltage source and the current in the small time-step side similarly transferred back to the large time step side, driving a current source branch.

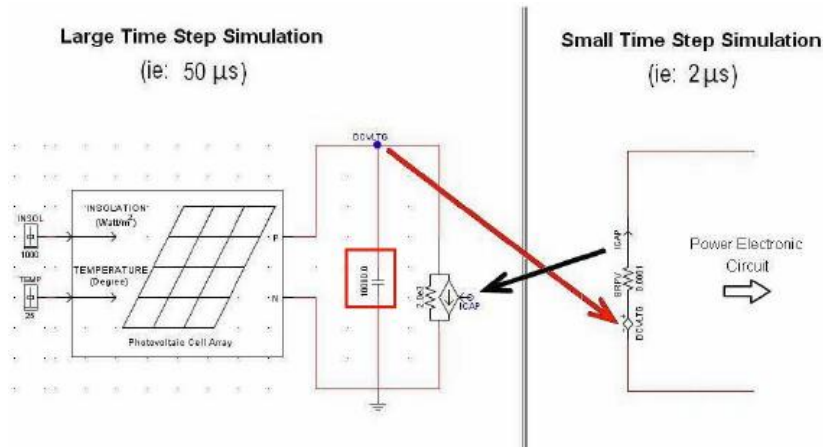


Figure 22: Large and small time-step simulation interface

The PV array is connected to the DC bus, and then to the AC grid via a DC/AC inverter. In the simulation, the firing pulses applied on the switching of the DC-AC inverters are determined by a comparison between a Controlled Sinusoidal Reference (CSR) and a triangular wave provided by the firing pulse generator component [73] , with Figure 47 presenting its control circuit. The inverter output voltage goes through a filtering stage and then is stepped up into a higher voltage level by three single-phase interface transformers that connect the main network and small time-step sub-network to the grid voltage at the point of common coupling. The grid equivalent is modelled as three-phase impedance based on the short circuit MVA in series with an ideal three-phase AC voltage source. The power is fed from PV system and the utility to the distribution network consisting of four step-down transformers. Tabulated in Table 5 are the PV system model parameters and the expected outputs at standard testing conditions (STC).

Table 5: PV system parameters and expected outputs at STC

Series modules	150
Parallel modules	300
Total number of modules	45000
Maximum power rating P_{max}	255 W
PV array Output power	11.47 MW
PV array Output voltage	5.670 kV

5.2.2. Steady-state operation

At the outset of the simulations, the PV model is run and the steady state voltages and currents observed at different temperature and insolation. The simulated system is first checked under STC (1000 W/m^2 and 25°C). Figure 23 illustrates the corresponding waveforms of electric characteristics for solar PV plant obtained from runtime in RTDS simulation.

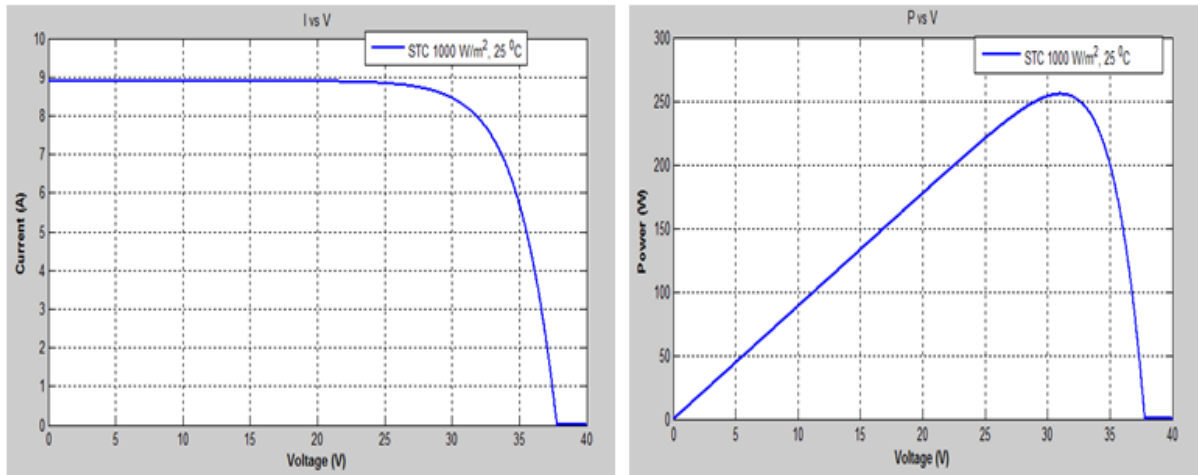


Figure 23: Characteristic curves of the PV array at STC

The curves have been generated by running the simulation and the results are very close to the manufacturer's curves, which imply that the PV panel has been modelled to adequate accuracy for fulfilling the requirement of this research. Figure 24 shows the PV array output voltage, the magnitude is found as expected shown in Table 5, corresponding to the chosen PV system parameters. With increase in irradiation, the solar panel output increases but with increase in ambient temperature, there is a relatively sharper reduction in the open circuit voltage (V_{oc}) of the panel than the slight increase in the short circuit current. Hence, the reduction in V_{oc} contributes to the reduction in overall panel power output.

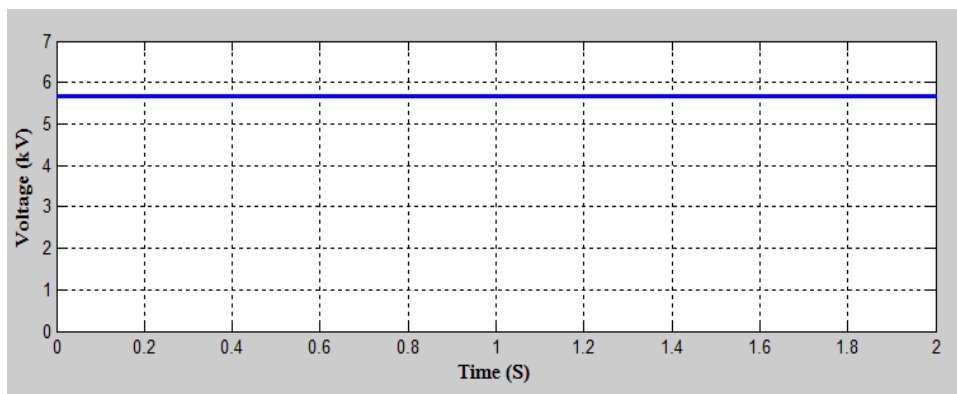


Figure 24: PV Array output voltage

Power supplied by the PV array into the inverter is 10.2 MW and the inverter outputs 10.18 MW with a 0.8 power factor. The maximum output power from the array under the stated conditions is relatively higher than the inverter output due to the estimation of the maximum power point and power losses in harmonics at the inverter output. A comparison has been made between the calculated theoretical power and the power obtained from RTDS simulation in respect of maximum insolation and maximum temperature. Apart from this, in real time, since the insolation and temperature variation occurs simultaneously, the rise in insolation results in increase in panel power output, but the rise in temperature exhibits a different behaviour and the net effect of rise in temperature is lowering the solar PV panel power output. The three-phase inverter converts the dc voltage to AC for grid interfacing and supply to the local load. The inverter output voltage is then filtered to remove the harmonic components, and then stepped up to match the voltage of the point of common coupling. Figure 25 shows the transformer output voltage that is connected to the 11 kV busbar.

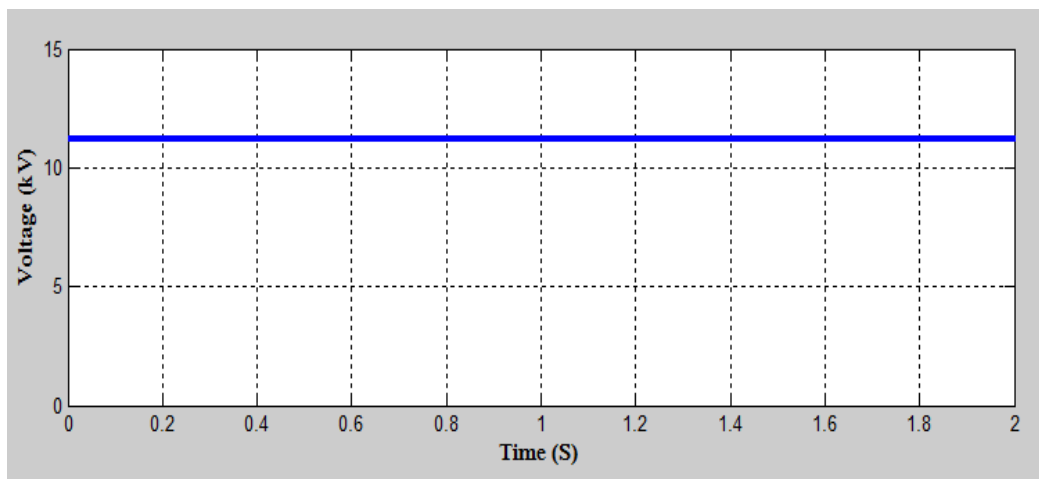


Figure 25: Stand-alone PV System output RMS voltage

The PV system output voltage is shown in Figure 25. The output power being fed to the grid has a small percentage dip with respect to the actual power generated by the solar PV array and this suppression of output power can be attributed to the losses in the converter and inverter. First, the simulations are carried out without inserting the DG into the network and all active and reactive power, voltage and current measurements are done. The simulation is then run with DG implemented into the network and the similar measurements done.

5.2.2.1 PV penetration at 11 kV

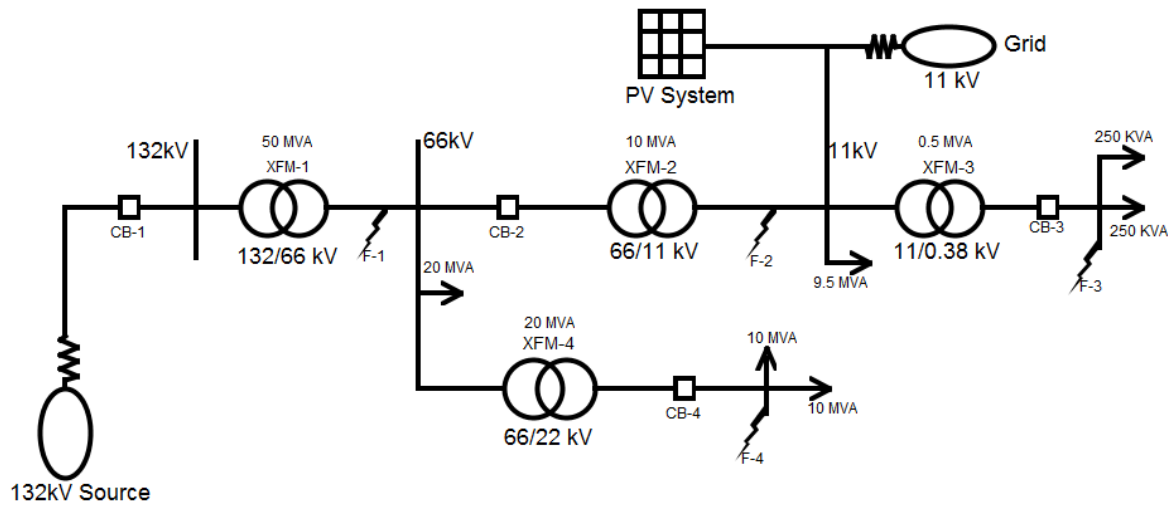


Figure 26: Single line diagram of the grid-tied photovoltaic system

The system chosen is the parallel operation of one PV generation renewable energy and a conventional grid represented as a constant voltage source behind short circuit impedance. The equivalent single diagram circuit of the system is shown in Figure 26, with PV generation, grid supply and rest of the network.

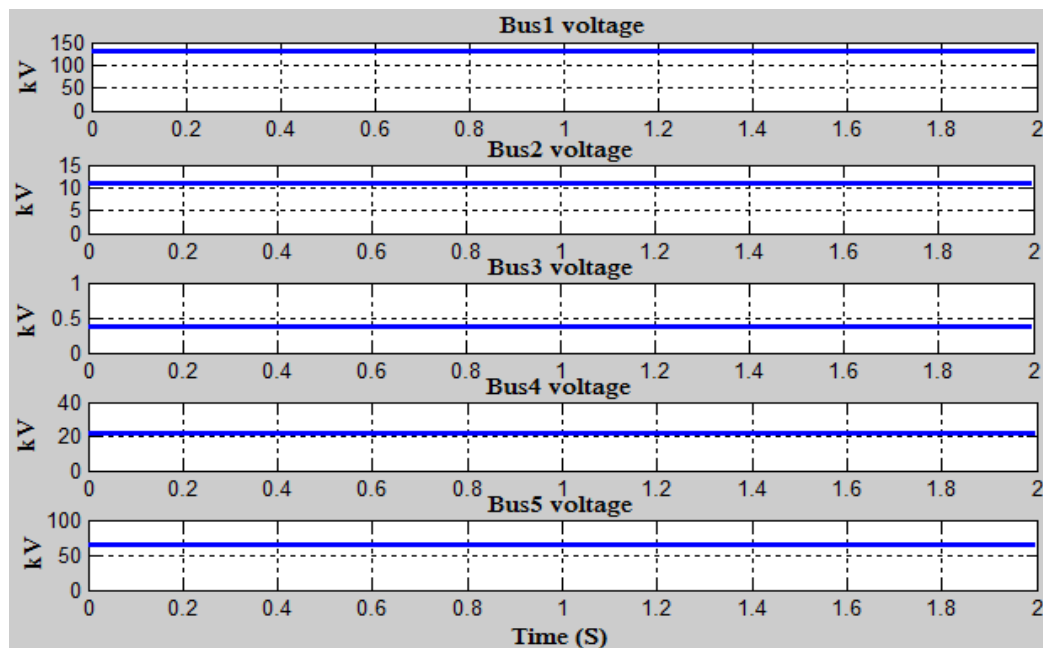


Figure 27: Grid-connected PV system voltages

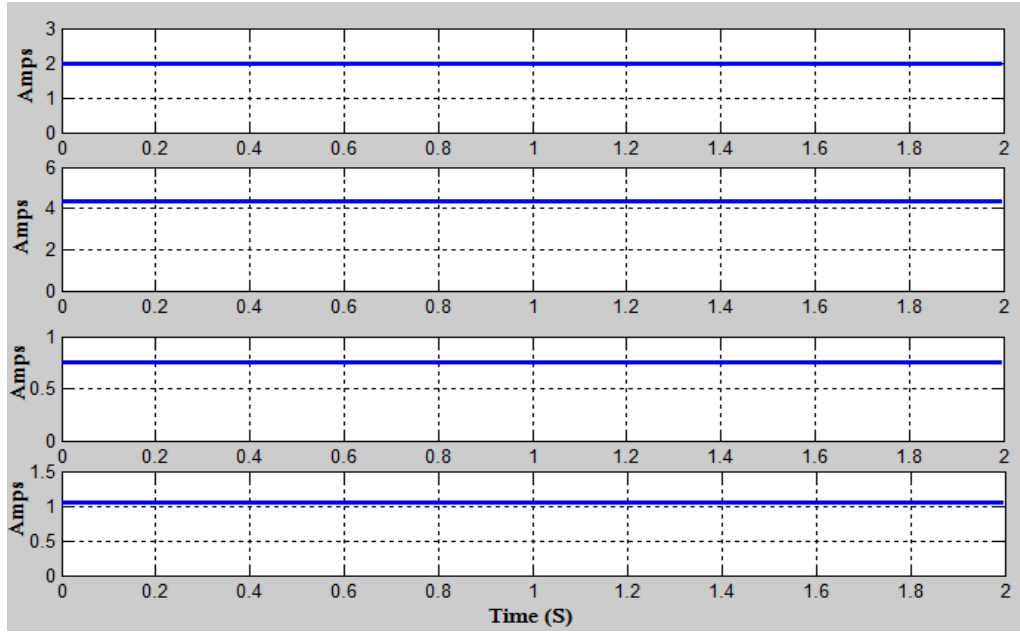


Figure 28: Grid-connected PV system CTs secondary RMS current

Figure 27 and Figure 28 show the system voltages and CTs secondary RMS currents 1 to 4 respectively after the PV system connection to the distribution network. As can be seen, current through CT-1 and CT-2 secondary windings is seen to have doubled and quadrupled respectively, and this can be accounted to the power being injected into the distribution system and backflow of current resulting from the addition of the PV generation system on the 11 kV busbar. The conditions met and results thus obtained are in accordance with the engineering principles in that the generated voltage of the incoming generator and the frequency of generated voltage connected in parallel to a busbar are equal to the busbar voltage and frequency.

5.2.2.2 PV penetration at 66 kV

Similarly, simulations are also carried out by varying the PV penetration level. The following results show the performance of the grid-connected PV system when point of common coupling is changed to the 66 kV busbar. As the PV penetration varies, the distribution feeders affected by the backflow of power change. The degree of impacts of DG addition to distribution systems is further illustrated in the following figures.

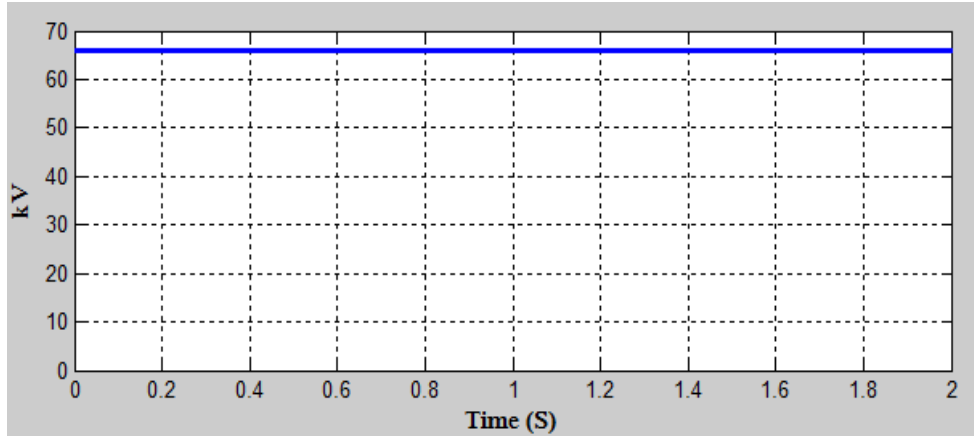


Figure 29: PV System RMS voltage

Figure 29 shows PV system output voltage before connection to the 66 *kV* busbar as the new point of common coupling. The PV system frequency and voltage are equal to the grid and busbar voltage and frequency.

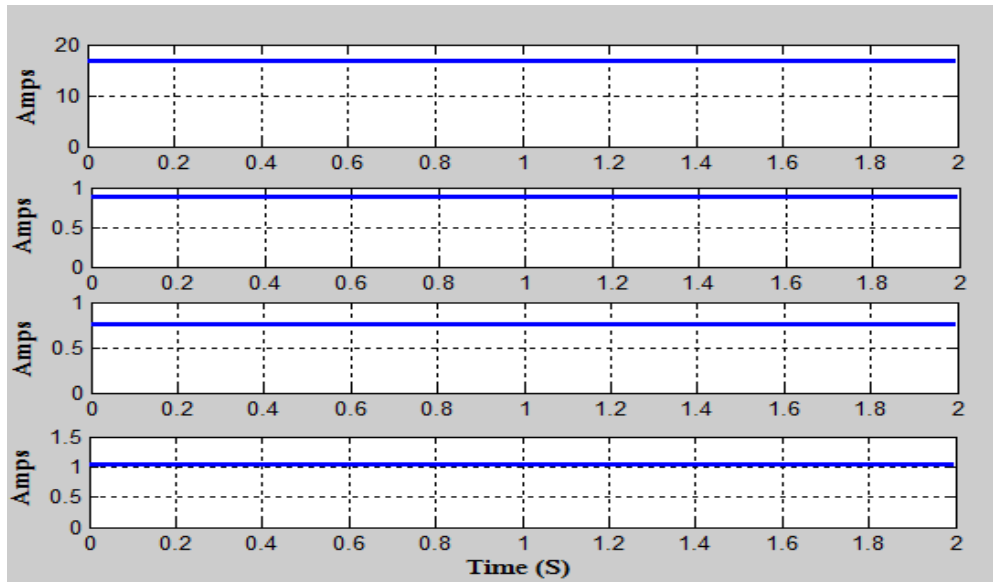


Figure 30: System RMS currents

According to [74], the reverse power flow is the main cause of current rise in distribution feeders. Figure 30 shows a summary of RMS currents observed on the network after the point of common coupling is changed to the 66 *kV* busbar. Due to the PV generation system, CT-1 secondary RMS current as seen in Figure 30 is 16.9 *Amps*, which is higher than the 1.05 *Amps* read in Figure 2 section 4.2 without the PV system. As the PV penetration increases, the real power supplied by the grid decreases, but the reactive power burden still remains wholly with the grid. The voltage rises at PCC when power is injected into the distribution system. PV inverters are capable of absorbing reactive power to mitigate voltage rise, just as they are capable of injecting reactive power in case of voltage sags [75].

5.2 Overcurrent Protection set-up

As stated earlier in the literature, injection of distributed generation to the conventional radial distribution networks poses challenges concerning the already existing system protection scheme. As soon as the fault takes place, it is sensed by both primary and backup protection. The primary protection is the first to operate, as its operating time is less than that of the backup relay. For the simple radial feeder shown under consideration, relay-3 should be the first to operate for fault F-3, followed by back-up relay-2 if it fails to operate. The challenge of coordination of overcurrent relays in distribution systems can be quantified as an optimization linear programming problem (LPP), whereby using dual simplex method, the operating times of the relays, for near end fault can be minimized [65], i.e.

$$\min z = \sum_{i=1}^m t_i \quad (2)$$

where t_i indicates the operating time of the primary relay at i , for near end fault. The objective is achieved under the following constraints:

A. Coordination criteria

$$t_{bi} - t_i \geq \Delta t \quad (3)$$

Where t_{bi} is the operating time of the backup relay for a fault at ' i ' and Δt is the coordination time interval (CTI).

B. Relay operating time boundaries

$$t_{imin} \leq t_i \leq t_{imax} \quad (4)$$

Where t_{imin} is the minimum operating time of relay and t_{imax} is the maximum operating time for the same relay.

C. Relay characteristics

Inverse definite minimum time (IDMT) characteristics are assumed to be same for all relays and plug setting taken as 1.

$$t_{op} = \frac{0.14}{PSM^{0.02} - 1} \times TMS \quad (5)$$

Where t_{op} is the time of operation, PSM is the plug setting multiplier and TMS is the time multiplier setting. Taking

$$a = \frac{0.14}{PSM^{0.02} - 1} \quad (6)$$

and substituting it into the objective equation (2), it becomes

$$\min z = \sum_{i=1}^m a_i (TMS)_i \quad (7)$$

$$PSM = \frac{\text{Fault Current}}{CT\text{-ratio}} \quad (8)$$

The dual simplex method algorithm used to solve the maximization problem is outlined in the methodology. Considering relay-1, relay-2 and relay-3, the minimum operating time for each relay is considered as 0.02 seconds and the CTI is taken as 0.4 seconds. The maximum fault currents at F-1, F-2 and F-3 are 52 kA, 500 kA and 930 kA respectively, with the CT ratios being set at 400:1, 500:1 and 1000:1 for relay 1, 2 and 3 respectively. Due to transformers XFM-1, XFM-2 and XFM-3 winding ratios, the fault currents seen by the circuit breakers CB-1, CB-2 and the relays' coils are less than the actual currents measured at the faulted points. The *PSM* and *a* values are calculated using equation (6) and (8), and are tabulated as shown in Table 6. PSM sample calculation for fault-3 current seen by relay-2 gives $I_{(3-2)} = 5354 \text{ A}$ and $PSM = 10.7$.

Table 6: PSM and *a* values

<i>Fault point and current</i>		<i>Relays</i>		
		<i>Relay-1</i>	<i>Relay-2</i>	<i>Relay-3</i>
F-1	<i>PSM</i>	65	-	-
52 kA	<i>a</i>	1.6	-	-
F-2	<i>PSM</i>	104	166.7	-
500 kA	<i>a</i>	1.43	1.29	-
F-3	<i>PSM</i>	-	10.7	930
930 kA	<i>a</i>	-	2.88	0.956

Adding slack variables and converting it into a maximization problem, the problem formulation is carried out using dual-simplex method as follows:

$$\text{Max } y = -1.6X_1 - 1.29X_2 - 0.956X_3$$

$$\text{Subject to: } -1.43X_1 + 1.290X_2 + S1 = -0.4$$

$$-2.88X_2 + 0.956X_3 + S2 = -0.4$$

$$-1.6X_1 + S3 = -0.02$$

$$-1.29X_2 + S4 = -0.02$$

$$-0.956X_3 + S5 = -0.02$$

The optimum solution is obtained in four basic iterations outlined in the appendix Table 8-11. At the end of fourth iteration, all the values in the last right-hand column are non-negative and the optimal solution is reached. The TMS values to be used are therefore 0.41 for relay-

1, 0.145 for relay-2 and 0.021 for relay-3. Due to the standard MiCOM P122 relay TMS settings, the values shall be taken as 0.45, 0.15 and 0.025 for relay 1, 2 and 3 respectively.

5.2.2 Experimentation results:

Of interest initially, is the adequate sequential relay operation. The calculated results are verified with an experimental model where the optimum relay TMS settings calculated in the previous section are set on and model simulations run. A positive correlation between the calculated results and proper relay coordination indicated by graphs from the simulations will give credence to the dual simplex method employed.

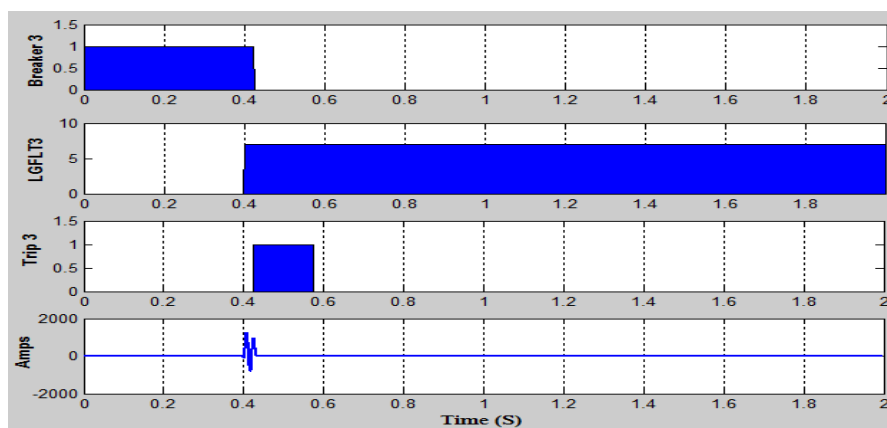


Figure 31: Relay-3 testing

Figure 31 shows results for relay-3 TMS validation. As expected, it can be seen from the plot that when a fault occurs, a trip signal is sent which consequently opens the circuit breaker immediately on the signal detection. The relay's time of operation was computed to be 0.023 *seconds*.

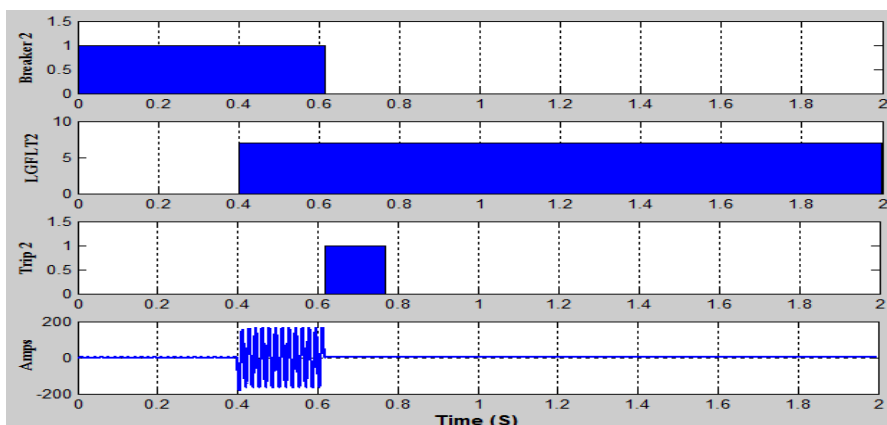


Figure 32: Relay-2 testing

In the same manner, the plot in Figure 32 shows successful operation of relay-2 with the TMS of 0.15 obtained using the dual simplex method. Computed from the graphs, relay-2 time of operation on fault F-2 occurrence is 0.72 *seconds*. For fault F-3, i.e. when relay-3 fails, relay-2 opens the circuit breaker in 1.12 *seconds*, which is 0.4 *seconds* later than relay-3 would have opened, thus honouring the coordination criteria presented by equation (3).

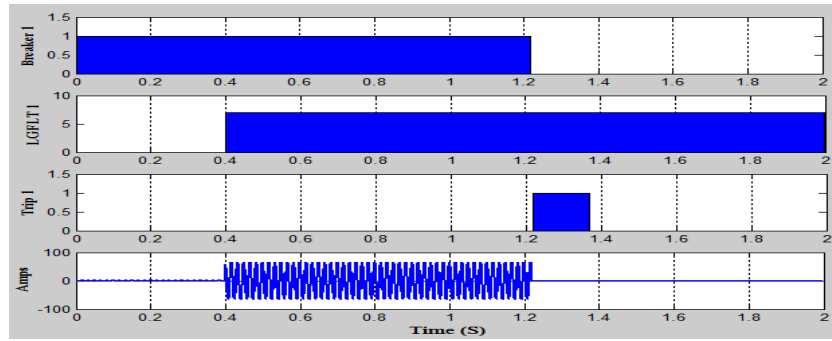


Figure 33: Testing relay-1

In Figure 33, relay-1 time of operation while using 0.45 TMS value obtained above is computed to be 0.805 *seconds*. From the simulations indicated in Figure 31 to Figure 33, relays 3, 2 and 1 times of operation are computed and they adhere to the constraints set in the dual simplex algorithm while solving the linear programming problem. This shows the optimum solution of time multiplier setting of relays was attained using dual simplex for the relays considered. The results also indicate that appropriate relay coordination for the distribution system under study was achieved. Taking into consideration relay-4 with a fault current of 95 *kA* and using the optimisation technique to compute the time multiplier setting:

$$PSM = \frac{95 \text{ kA}}{500:1} = 190, \text{ giving } a = 1.26$$

$$\text{Min } y = 1.26X_1, \text{ subject to } 1.26X_1 \geq 0.02$$

Applying the similar dual simplex method as performed above gives a TMS of 0.015

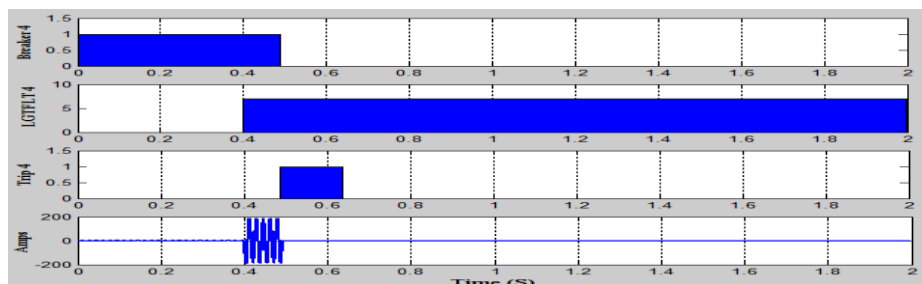


Figure 34: Relay-4 testing results

Figure 34 gives the operation time of relay-4 as 0.088 *seconds*, and further simulations show that when relay-4 fails, relay-1 operates in 0.94 *seconds*, indicating that accurate and optimum solutions were achieved for the overall system relays' coordination.

5.3 Islanding Protection

Islanding of a grid connected distributed generation (DG) occurs when a section of the utility system containing such generators is disconnected from the main utility, but the independent DGs continue to energize the utility lines in the isolated section (termed as an island) [76]. Unintended islanding is a concern primarily because it poses a hazard to utility and customer equipment, maintenance personnel, and the general public; hence, anti-islanding protection is essential to ensure that grid-tied energy harvesting systems cut their connection to the grid when the grid itself loses power. The identification of power loss in the grid can be challenging, requiring an approach able to find the right balance between sensitivity to normal fluctuations in the grid and responsiveness to grid power failure. Many anti-islanding techniques have been proposed to prevent islanding caused by DGs [77] [78]. They are either passive techniques that monitor the voltage and frequency or active methods where the output of the reactive power is varied to help destabilize the island and accelerate the dissolving of the system to extinguish the island.

5.3.2 Passive techniques

a) Under/Over voltage and Under/Over frequency

Under/Over voltage and Under/Over frequency relaying are effective loss of grid (LOG) techniques for small DGs. According to [67], they usually provide an acceptable level of protection but may fail to operate if the change of load associated with LOG can be compensated by the DGs' control system, keeping voltage and frequency more or less stable.

b) Rate of change of frequency (ROCOF)

ROCOF relays monitor the voltage waveform and trips the CB when the measured rate of change of frequency exceeds a pre-set level for longer than a set period [68]. The settings are chosen such that the relay operates only for fluctuations associated with islanding and with the DG operating independently from the utility, but not for those fluctuations governed by utility time constants [67].

5.3.3 Active techniques

a) Reactive power export error detection

A level of reactive power flow in the inter-tie between the DG and the utility is generated by DG control system interfaced with the reactive power export error detection relay. This level can only be maintained when the utility generation is connected. There should be a considerable reduction on the DG disturbance during normal operation and has to, after islanding, be sufficient to drive the frequency outside its threshold limits [67] [79]. The relay operates when there is an error between the setting and the actual reactive power being exported for a period greater than the set value.

b) System fault level monitoring

In this scheme, system fault level is monitored by sensing the short circuit current and reduction in supply voltage when a shunt inductor is connected across the supply by using point-on-wave triggered, thyristor switches. It is a faster acting protection technique. Its tripping is dependent on the power system's source impedance close to the inter-tie. Firing of the thyristor occurs just before a current zero [80]. This causes a short pulse of current to flow in the inductor and a voltage glitch. The tripping decision depends on the comparison of the measured system fault level with that corresponding to a network fed from the utility generation [67].

5.3.4 Islanding operation

The difficulties with islanded DG have been outlined in the literature review. To prevent island operation, the protection system has to detect islands quickly and reliably. Much literature is available concerning protection of distributed generation. Many publications demonstrate the same problems and issues, but solutions are rare.

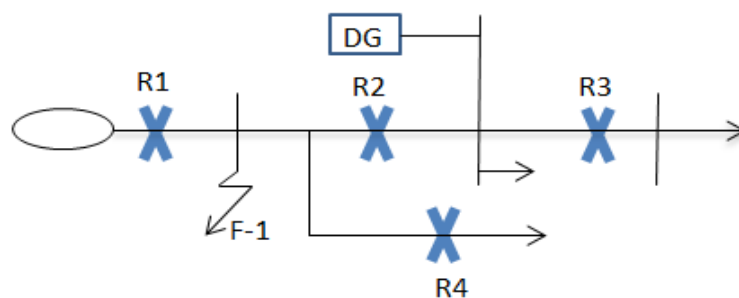


Figure 35: A radial feeder with PV generation integrated

Figure 35 shows a simple single line diagram of the distribution feeder modelled with a fault F-1 applied nearer to the source. As soon as the fault takes place, it is sensed by relay R1

which then trips and opens the circuit breaker CB-1 shown in Figure 26. Due to the location of the fault, the source is cut from and does not supply the grid; however, the PV generation system denoted by DG is still connected to the rest of the network, resulting in an island.

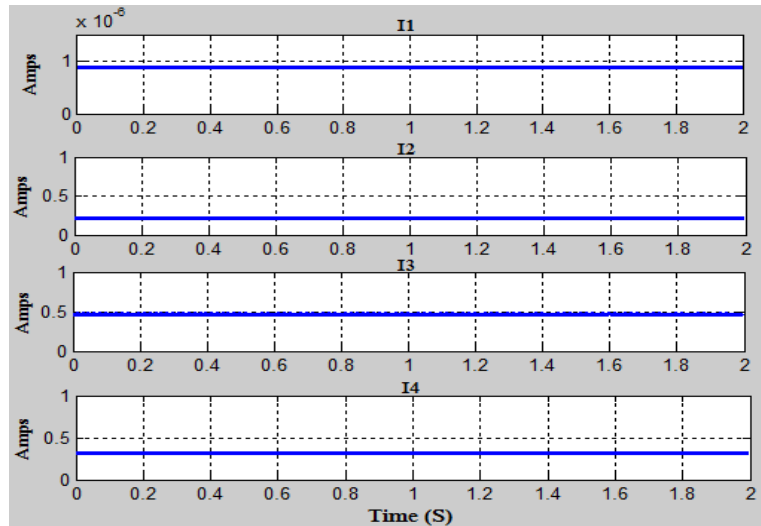


Figure 36: Distribution system currents due to islanding

Figure 36 indicates network RMS currents after experiencing fault F-1. The utility protection system detected the overcurrent and opened circuit breaker CB-1, and as can be seen, there is almost no phase RMS current I_1 flowing in the 132 kV feeder, 0.9×10^{-6} Amps. Although the source is disconnected from the rest of the network, the PV system still supplies the grid and hence current I_2 , I_3 and I_4 flows. In the context of power supply to loads, there is current flowing but the condition is unfavourable as critical situations can occur due to the part of the utility network which is islanded and the connected integrated PV unit.

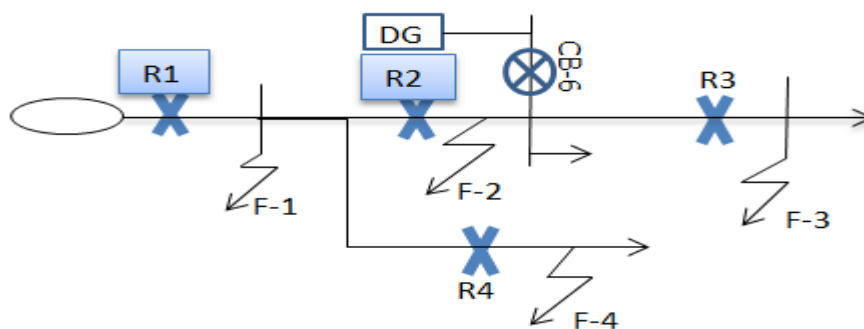


Figure 37: Protection against islanding layout

An example of a simple protection technique against islanding is shown in Figure 37. The overcurrent protection relays R1 and R2 provide basic detection of faults that will separate the DG from the utility by opening circuit breaker CB-6 if fault F-1 or F-2 occurs. The circuit breaker is controlled by a trip signal from either R1 or R2.

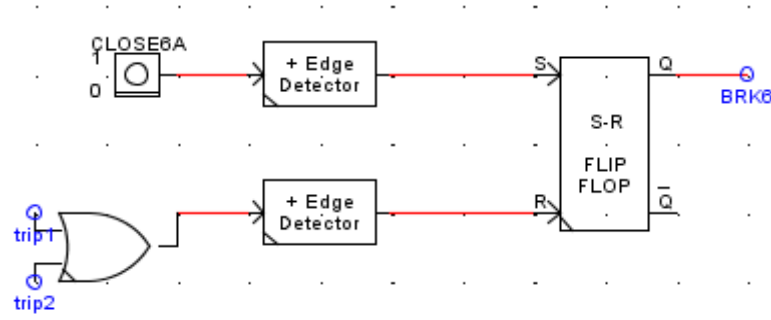


Figure 38: Circuit breaker logic

Shown in Figure 38 is the logic used to control the breaker. As can be seen, the logic circuit has both trip1 and trip2 signals as inputs. In the system, once either relay R1 or R2 has issued a trip command to the breaker logic shown, the circuit breaker receives the signal from the S-R latch to open and it remains open until manually closed by pressing of a ‘close’ push button in runtime. The circuit breaker model is designed to respond to separate open and close commands by means of an SR flip-flop component. When F-1 occurs, relay R1 sends a trip signal that governs both circuit breaker CB-1 and CB-6, disconnecting the source and distributed generation from the main utility network as shown in Figure 39. For fault F-2 shown in Figure 41, a similar phenomenon takes place where CB-2 and CB-6 open, leaving the R4 feeder branch connected to the source and load being supplied. In the event of fault F-3 or F-4 occurring, trip signals are sent from R3 and R4 respectively to open corresponding circuit breakers, leaving the source and PV generation system connected to the utility.

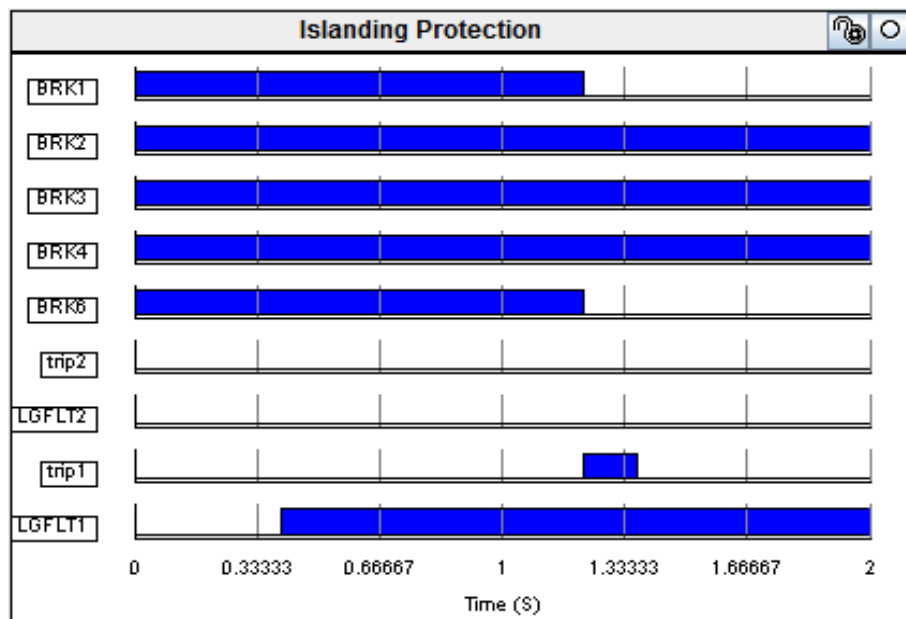


Figure 39: Circuit breaker 1 and 6 opening on fault F-1 occurrence

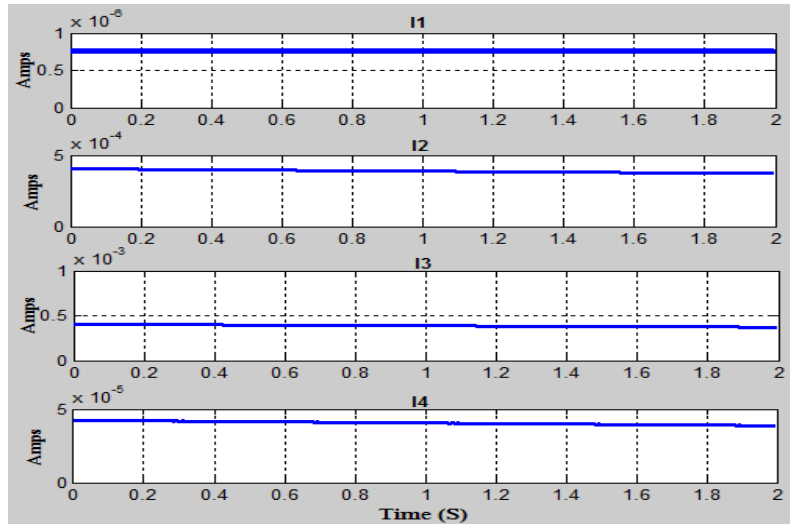


Figure 40: System line current during islanding protection

Figure 40 shows the distribution system line currents after fault F-1 occurs. Due to the open circuit breakers disconnecting both the source and PV system from the grid, there is almost no current flowing since the system is not getting any voltage supply.

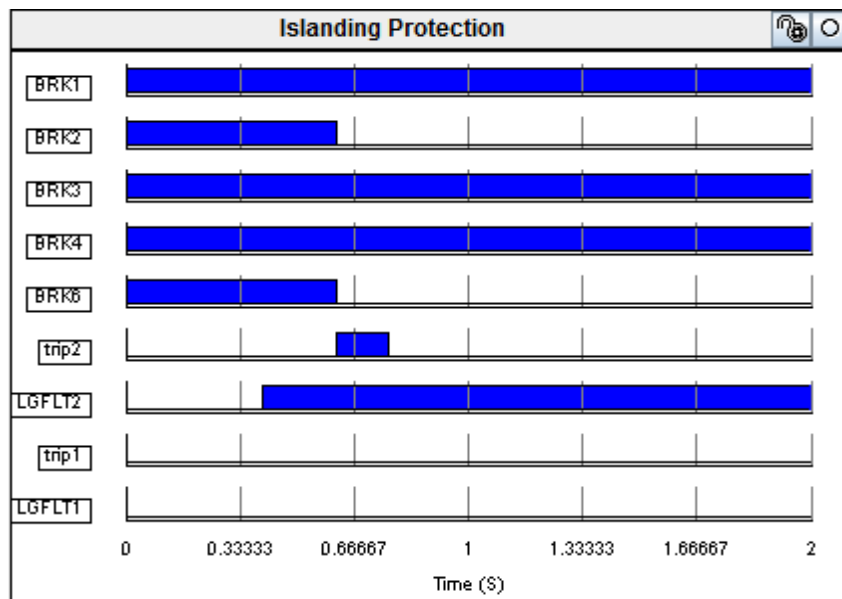


Figure 41: Circuit breaker 1 and 6 opening on fault F-2 occurrence

For safety concerns, a successful implementation of anti-islanding assists against unexpected live wires, which repair crews may be faced with during a fault or maintenance. End-user equipment is also guarded against damage since customer equipment could theoretically be damaged if operating parameters differ greatly from the normal.

6 Conclusion

Apart from fossil fuels that power thermal power plants, alternative fuels are under consideration due to the rising electrical energy demand. This led to the development of innovative electrical power distribution systems where photovoltaic generation systems supply some of the energy and centralized generation produces some. Major concerns relating to penetration of PV systems included poor relay coordination, sympathetic tripping and unintentional islands that result from continuous power flow from the dispersed generation systems although the grid is disconnected during a fault. This work involved modelling and development of an overcurrent protection scheme for a modified test distribution network with and without dispersed generation. A study of the electricity distribution systems was done and the system model developed. All the relevant theory prior to the technical design and all results obtained thus far in terms of the design procedure progress were discussed. This research work presented the experimental results of the protection scheme using both software and hardware relays on RTDS. Control logic functions for system faults and circuit breakers were implemented and tested on all protection zones and the obtained results demonstrated correct operation. The expected relay operation defined in the theory was verified, with the higher fault currents showing a reduction in relay time of operation. The results were discussed and analyzed to verify existing theories under steady and faulted operating conditions.

Integration of all parts of the work with physical components to obtain a system where the complete protection philosophy was implemented. The RTDS enables hardware closed-loop testing with the distribution system digital model. Results were compared with the theoretical values obtained from manual calculations, which as expected were approximately equal with percentage deviations below 3%. The results show a relatively higher time of operation for hardware relays as compared to using software relays. The adjusted time multiplier setting when using hardware relays and the possibility of delays from the amplification stage influenced the discrepancies in the relay time of response since physical relays use a certain TMS values range and standard settings so some values could not be used exactly as manually calculated. Coordination of the protection relays was tested on the distribution system and implemented using the software and hardware relays in verification of the relay coordinated sequential operation during faults. The test system was analysed without the presence of DG, which served as a basis with which subsequent results were compared to.

The research focus was also on the study of DG impacts on the fault current and voltage of the overall protection scheme for the distribution systems. Described were the PV model fundamentals, I-V characteristic and its output dependency on temperature and solar irradiance. Simulations in chapter 5 indicated that PV systems affect fault current and voltage in the distribution systems by changing the direction and magnitude of the fault current in the network and these impacts differ depending on the penetration location. Due to the impacts, the radial distribution systems original protection schemes did not hold anymore hence the need for an adaptive protection scheme to accommodate DG penetration. Chapter 2 discussed a number of mitigation methods to the impacts on radial distribution systems overcurrent protection. The investigation concluded that the inverter-interfaced PV systems' fault current contribution is relatively low but it does however disturb the present protection coordination, and suggested a method for modifying the TMS to meet the requirements of correct relay discrimination. Some of the methods were found to be rather complicated and not efficient. To address mainly the issue of relay coordination, which is considered a highly constrained optimization problem, a dual simplex method optimization algorithm was implemented for time multiplier settings computation and the objective achieved. Lastly, after the simulation and ensuring correct and efficient sequential relay operation, the issue of unintentional islanding had to be investigated and solved. The next step involved developing an interconnection protection method to protect against the issue of islanding. A modified adaptive protection scheme's functionality was successfully implemented and verified on the interconnected distribution network. For huge volumes of PV units, the control logic used would have to be modified to accommodate the network under consideration.

Future recommendations

With future inclinations and within the electric power delivery field, wide-ranging view is that dispersed generation is anticipated to play a significant role in future energy systems. There is a global increasing demand for alternative renewable energy sources and its storage, which is fast gaining importance in today's developments. Further recommendations would be to study extensively the distributed generation protection and stability analysis along with islanding and implementation of more effective anti-islanding techniques. Moreover, studies can be carried out on protection with distinct emphasis on operation and re-synchronization of islanded parts of distribution systems. Since there is a lot of exciting research in the field of renewable energy and control systems, the future work should also be on future design of distribution networks for a simplified DGs interconnection.

References

- [1] A. Evans and V. Strezov, "A Sustainability Assessment of Electricity Generation," in *2010 International Conference on Biosciences*, Mexico, 2010.
- [2] Z. Li, "Natural gas for generation: a solution or a problem?," *IEEE Power and Energy Magazine*, vol. 3, no. 4, pp. 16 - 21, 2005.
- [3] N. K. Choudhary, . R. S. Mohanty and . K. R. Singh, "Protection Coordination of Over Current Relays in distribution system with DG and superconducting fault current limiter," in *2014 Eighteenth National Power Systems Conference*, Guwahati, 2014.
- [4] J. Franco, . L. Ochoa and . R. Romero, "AC OPF for Smart Distribution Networks: An Efficient and Robust Quadratic Approach," *IEEE Transactions on Smart Grid*, no. 99, pp. 1-1, 2017.
- [5] D. Chengdi, L. Peng, W. Chengshan, W. Zhiying, Y. Dawei, Z. Jin and L. Zheng, "A design and implementation of FPGA-based real-time simulator for distribution system with DG integration," in *2016 China International Conference on Electricity Distribution (CICED)*, Xi'an, 2016.
- [6] M. Monadi, A. M. Zamanic, J. Ignacio , C. Alvaro and L. Pedro, "Protection of AC and DC distribution systems Embedding distributed energy resources: A comparative review and analysis," *Renewable and Sustainable Energy Reviews*, vol. 51, pp. 1578-1593, 2015.
- [7] F. Coffele, C. Booth and A. Dyśko, "An Adaptive Overcurrent Protection Scheme for Distribution Networks," *IEEE Transactions On Power Delivery*, vol. 30, no. 2, pp. 561-568, 2015.
- [8] Rakesh Sinha and A. Zaidi, "Protection of Distribution Systems with Significant Penetration of Distributed Generation," in *Power Generation System and Renewable Energy Technologies*, Karachi, 2015.
- [9] G. Electric, "Distribution System Feeder Overcurrent Protection," GE Power Management, Canada.
- [10] F. B. Costa, A. Monti and S. C. Paiva, "Overcurrent Protection in Distribution Systems with Distributed Generation based on the Real-Time Boundary Wavelet Transform," *IEEE Transactions on Power delivery*, vol. 32, no. 1, pp. 462-473, 2017.
- [11] J. M. Gers and E. J. Holmes, Protection of electricity distribution networks, London: The Institution of Electrical Engineers, 1998.
- [12] S. Behzadiraifi and H. Salehfar, "Preventive Maintenance Scheduling Based on Short Circuit and Overload Currents," *IEEE Transactions on Smart Grids*, vol. 6, no. 4, pp. 1740-1747, 2015.
- [13] M. Lantz, "Fault-Resistance Effect on Ground Fault Current," *AIEE Transactions*, vol. 72, 1953.
- [14] S. H. Horowitz and A. G. Phadke, Power System Relaying, England: Research Studies Press LTD., 1995.
- [15] B. Ram and N. D. Vishwakarma, Power System Protection and Switchgear, New Delhi: McGraw Hill Education Private Limited, 2011.

- [16] L. J. Blackburn, Protective Relaying Principles and Applications, New York: Marcel Dekker Inc, 1998.
- [17] IEEE, “Reducing Outages Through Improved Protection, Monitoring, Diagnostics, and Autorestation in Transmission Substations—(69 kV and Above),” *IEEE Transactions On Power Delivery*, vol. 31, no. 3, pp. 1327-1334, 2016.
- [18] B. Ravindranath and M. Chander, Power system protection and switchgear, New Delhi: New Age International Publishers, 1995.
- [19] T. Guillod, F. Krismer and J. W. Kolar, “Protection of MV Converters in the Grid: The Case of MV/LV Solid-State Transformers,” *IEEE Journal of Emerging and Selected Topics in Power Electronics*, vol. 5, no. 1, pp. 393 - 408, 2017.
- [20] Y. G. Paithankar and . S. R. Bhide, Fundamentals of Power System Protection, India: PHI Learning, 2011.
- [21] A. Onal, “Relay coordination in the protection of radially connected power system network,” *Nigerian Journal of Technology* , vol. 31, pp. 58-62, 2012.
- [22] A. F. Sleva, Protective Relay Principles, Boca Raton: Taylor & Francis Group, 2009.
- [23] B. Ram and P. N. Vishwakarma, Power System Protection and Switchgear, India: McGraw-Hill Education Private Limited, 2011.
- [24] B. Feizifar and O. Usta, “Condition monitoring of circuit breakers: Current status and future trends,” in *2017 IEEE International Conference on Environment and Electrical Engineering and 2017 IEEE Industrial and Commercial Power Systems Europe*, Milan, 2017.
- [25] J. McCalley, O. Oluwaseyi, V. Krishnan and R. Dai , “System Protection Schemes: Limitations, Risks, and Management,” Power Systems Engineering Research Center, Texas, 2010.
- [26] L. Sevov, U. Khan and Z. Zhang, “Enhancing power transformer differential protection to improve security and dependability,” *IEEE Transactions on Industry Applications*, vol. 53, no. 3, pp. 2642 - 2649, 2017.
- [27] Y. Yin, Z. Zhang and Y. Fu, “A bus differential protection scheme using real-time synchrophasor data,” in *2017 IEEE 30th Canadian Conference on Electrical and Computer Engineering (CCECE)*, Windsor, 2017.
- [28] C. Edward, O. I. Okoro and T. M. Khan, Concise Higher Electrical Engineering, Cape Town: Juta and Company Ltd, 2008.
- [29] Areva, Network Protection and Automation Guide, Barcelona: Cayfosa, 2005.
- [30] C. So, K. Li, K. Lai and K. Fung, “Application of genetic algorithm for overcurrent relay coordination,” in *Sixth International Conference on Developments in Power System Protection*, Nottingham, 1997.
- [31] A. Sinclair, D. Finney, D. Martin and P. Sharma, “Distance Protection in Distribution Systems: How It Assists With Integrating Distributed Resources,” *IEEE TRANSACTIONS ON INDUSTRY APPLICATIONS*, vol. 50, no. 3, pp. 2186-2196, 2014.

- [32] P. Mahat, Z. Chen, B. Bak-Jensen and C. . L. Bak, "A Simple Adaptive Overcurrent Protection of Distribution Systems With Distributed Generation," *IEEE Transaction on Smart Grid*, vol. 2, no. 3, pp. 428-437, 2011.
- [33] N. Gaur and P. Gaur, "Automation in Power Distribution Systems," *Journal of Engineering Research and Studies*, vol. 3, no. 2, pp. 82-84, 2012.
- [34] V. Prasad, . P. Rao and . S. Rao, "Coordination of directional relays without generating all circuits," *IEEE Transactions on Power Delivery*, vol. 6, no. 2, pp. 584 - 590, 1991.
- [35] D. A. Ko, G. Burt, S. Galloway, C. Booth and J. McDonald, "UK distribution system protection issues," *IET Generation, Transmission & Distribution*, vol. 1, no. 4, pp. 679 - 687, 2007.
- [36] D. Jones, Analysis and Protection of Electrical Power Systems, Great Britain: Pitman, 1996.
- [37] A.-M. Borbely and J. F. Kreider, Distributed Generation: The Power Paradigm for the New Millennium, Boca Raton: CRC Press, 2001.
- [38] A. K. Singh and S. K. Parida, "Need of distributed generation for sustainable development in coming future," in *2012 IEEE International Conference on Power Electronics, Drives and Energy Systems*, Bengaluru, 2012.
- [39] P. M. Sotkiewicz and I. J. M. Vignolo, "Nodal pricing for distribution networks: efficient pricing for efficiency enhancing DG," *IEEE Transactions on Power Systems*, vol. 21, no. 2, pp. 1013 - 1014, 2006.
- [40] T. Wang, D. O'Neill and H. Kamath, "Dynamic Control and Optimization of Distributed Energy Resources in a Microgrid," *IEEE Transactions on Smart Grid*, vol. 6, no. 6, pp. 2884 - 2894, 2015.
- [41] H. Jiayi, J. Chuanwen and X. Rong, "A review on distributed energy resources and MicroGrid," *Renewable and Sustainable Energy Reviews*, vol. 12, no. 9, pp. 2472-2483, 2008.
- [42] T. Bradford, Solar revolution: the economic transformation of the global energy industry, Cambridge: MIT Press, 2006.
- [43] C. A. Langston and G. K. C. Ding, Sustainable Practices in the Built Environment, Oxford: Routledge, 2008.
- [44] F. L. Luo and H. Ye, Renewable Energy Systems: advanced conversion technologies and applications, Boca Raton: CRC Press, 2013.
- [45] S. Kouro, J. I. Leon, D. Vinnikov and L. G. Franquelo, "Grid-Connected Photovoltaic Systems: An Overview of Recent Research and Emerging PV Converter Technology," *IEEE Industrial Electronics Magazine*, vol. 9, no. 1, pp. 47 - 61, 2015.
- [46] L. Stoyanov and N. Cholakova, "Simulation of the shading in photovoltaic systems," in *2017 15th International Conference on Electrical Machines, Drives and Power Systems*, Bulgaria, 2017.
- [47] R.-J. Wai and W.-H. Wang, "Grid-Connected Photovoltaic Generation System," *IEEE Transactions on Circuits and Systems*, vol. 55, no. 3, pp. 953-964, 2008.

- [48] I. H. Altas and A. Sharaf, "A Photovoltaic Array Simulation Model for Matlab-Simulink GUI Environment," in *2007 International Conference on Clean Electrical Power*, Capri, 2007.
- [49] J. Sreedevi, N. Ashwin and N. Raju, "A Study on Grid Connected PV system," in *2016 National Power Systems Conference (NPSC)*, Bhubaneswar, 2016.
- [50] P. T. Manditereza and R. Bansal, "Renewable distributed generation : The hidden challenges – A review from the protection perspective," *Renewable and Sustainable Energy Reviews*, vol. 58, p. 1457–1465, 2016.
- [51] S. Conti, "Analysis of distribution network protection issues in presence of dispersed generation," *Electric Power Systems Research*, vol. 79, no. 1, pp. 49-56, 2009.
- [52] H. A. Abdel-Ghany, M. Ahmed , N. I. Elkalashy and E. M. Rashad, "Optimizing DG penetration in distribution networks concerning protection schemes and technical impact," *Electric Power Systems Research*, vol. 128, pp. 113-122, 2015.
- [53] D. M. Laverty, . R. J. Best and D. J. Morrow , "Loss-of-mains protection system by application of phasor measurement unit technology with experimentally assessed threshold settings," *IET Generation, Transmission & Distribution*, vol. 9, no. 2, pp. 146-153, 2015.
- [54] H. Zayandehroodi, . A. Mohamed, H. Shareef and M. Mohammadjafari, "Impact of distributed generations on power system," *International Journal of the Physical Sciences*, vol. 6, no. 16, pp. 3999-4007, 2011.
- [55] T. M. Masaud and R. D. Mistry, "Fault current contribution of Renewable Distributed Generation: An overview and key issues," in *2016 IEEE Conference on Technologies for Sustainability*, Phoenix, 2016.
- [56] N. K. Roy and H. R. Pota, "Current Status and Issues of Concern for the Integration of Distributed Generation Into Electricity Networks," *IEEE Systems Journal*, vol. 9, no. 3, pp. 933 - 944, 2015.
- [57] Y. Pan, I. Voloh and W. Ren, "Protection issues and solutions for protecting feeder with distributed generation," in *2013 66th Annual Conference for Protective Relay Engineers*, College Station, 2013.
- [58] H. Teng, C. Liu, M. Han, S. Ma and X. Guo, "IEEE9 Buses System Simulation and Modeling in PSCAD," in *2010 Asia-Pacific Power and Energy Engineering Conference*, Chengdu, 2010.
- [59] K. G. Ravikumar, N. N. Schulz and A. K. Srivastava, "Distributed simulation of power systems using real-time digital simulator," in *2009 IEEE/PES Power Systems Conference and Exposition*, Seattle, 2009.
- [60] M. D. O. Faruque, T. Strasser, G. Lauss, V. Jalili-Marandi, P. Forsyth, C. Dufour, V. Dinavahi, A. Monti, P. Kotsampopoulos, J. A. Martinez, K. Strunz, M. Saeedifard, X. Wang, D. Shearer and M. Paolone, "Real-Time Simulation Technologies for Power Systems Design, Testing, and Analysis," *IEEE Power and Energy Technology Systems Journal*, vol. 2, no. 2, pp. 63 - 73, 2015.
- [61] U. Rudež, P. Osredkar and R. Mihalič, "Overcurrent protection-relay testing with Real-Time Digital Simulator Hardware," in *Elektrotehniski Vestnik*, Slovenia, 2012.
- [62] D. Rayworth and M. A. Rahim, "Configuration and Setting of Protection Relays or Numeric

- Relays,” in *The IEE Seminar on Advances in Power Protection: Learning the Lessons from Major Disturbances*, London, 2006.
- [63] T. T. Trung, S.-J. Ahn and J.-H. Choi, “Real Time Simulation of Distribution System with Distributed Energy Resources,” *Journal of Clean Energy Technologies*, vol. 3, no. 1, pp. 57-61, 2015.
- [64] M. G. Villalva, J. R. I. Gazoli and E. R. Filho, “Comprehensive Approach to Modeling and Simulation of Photovoltaic Arrays,” *IEEE Transactions on Power Electronics*, vol. 24, no. 5, pp. 1198 - 1208, 2009.
- [65] P. P. Bedekar, S. R. Bhide and V. S. Kale, “Optimum Coordination of Overcurrent Relays in Distribution System Using Dual Simplex Method,” in *International Conference on Emerging Trends in Engineering & Technology*, Nagpur, 2009.
- [66] A. Gupta, . G. O. Swathika and S. Hemamalini, “Optimum Coordination of Overcurrent Relays in Distribution Systems Using Big-M and Dual Simplex Methods,” in *International Conference on Computational Intelligence and Communication Networks*, Jabalpur, 2015.
- [67] S. Chowdhury, S. Chowdhury, C. F. Ten and P. Crossley, “Islanding protection of distribution systems with distributed generators — A comprehensive survey report,” in *2008 IEEE Power and Energy Society General Meeting - Conversion and Delivery of Electrical Energy in the 21st Century*, Pittsburgh, 2008.
- [68] X. Ding and P. A. Crossley, “Islanding detection for distributed generation,” *Journal of Electrical Engineering and Technology*, vol. 2, no. 1, pp. 19-28, 2007.
- [69] A. J. Onal, “Relay Coordination in The Protection Of Radially-Connected Power System,” *Nigerian Journal of Technology*, vol. 31, no. 1, pp. 58-62, 2012.
- [70] A. Kamal, S. Sankar and R. Soundarapandian, “Optimal Over Current Relay Coordination of a Real Time Distribution System with Embedded Renewable Generation,” *Indian Journal of Science and Technology*, vol. 7, no. 7, pp. 149-155, 2014.
- [71] P. G. McLaren, R. Kuffei, R. Wierck, J. Giesbrecht and L. Arendt, “A Real Time Digital Simulator For Testing Relays,” *Transactions on Power Delivery*, vol. 7, no. 1, pp. 207-213, 1992.
- [72] J. Ahmad, “A fractional open circuit voltage based maximum power point tracker for photovoltaic arrays,” in *International Conference on Software Technology and Engineering*, San Juan, 2010.
- [73] G. G. Pinheiro, J. M. d. C. Filho and . D. B. Bonatto, “Modeling, simulation and comparison analysis of an installed photovoltaic system using RTDS,” in *IEEE International Conference on Industry Applications*, Brazil, 2016.
- [74] H. Mortazavi, H. Mehrjerdi, M. Saad and D. Asber, “A Monitoring Technique for Reversed Power Flow Detection With High PV Penetration Level,” *IEEE Transactions on Smart Grid*, vol. 6, no. 5, pp. 2221 - 2232, 2015.
- [75] J. Sreedevi, N. Ashwin and N. M. i Raju, “A study on grid connected PV system,” in *2016 National Power Systems Conference*, Bhubaneswar, 2016.

- [76] V. John, Z. Ye and A. Kolwalkar, "Investigation of anti-islanding protection of power converter based distributed generators using frequency domain analysis," *IEEE Transactions on Power Electronics*, vol. 19, no. 5, pp. 1177 - 1183, 2004.
- [77] R. J. Bravo, S. A. Robles and . E. Muljadi, "Assessing solar PV inverters' anti-islanding protection," in *IEEE 40th Photovoltaic Specialist Conference*, Denver, 2014.
- [78] G. Smith, P. Onions and D. Infield, "Predicting islanding operation of grid connected PV inverters," *IEE Proceedings - Electric Power Applications*, vol. 147, no. 1, pp. 1 - 6, 2000.
- [79] X. Chen and Y. Li, "An Islanding Detection Method for Inverter-Based Distributed Generators Based on the Reactive Power Disturbance," *IEEE Transactions on Power Electronics*, vol. 31, no. 5, pp. 3559 - 3574, 2016.
- [80] J. Berry, S. Jupe, M. Meisinger and J. Outram, "Implementation of an active fault level monitoring system for distributed generation integration," in *22nd International Conference and Exhibition on Electricity Distribution*, Stockholm, 2013.

Appendix

A. Distribution system:

A RSCAD model of the distribution system network:

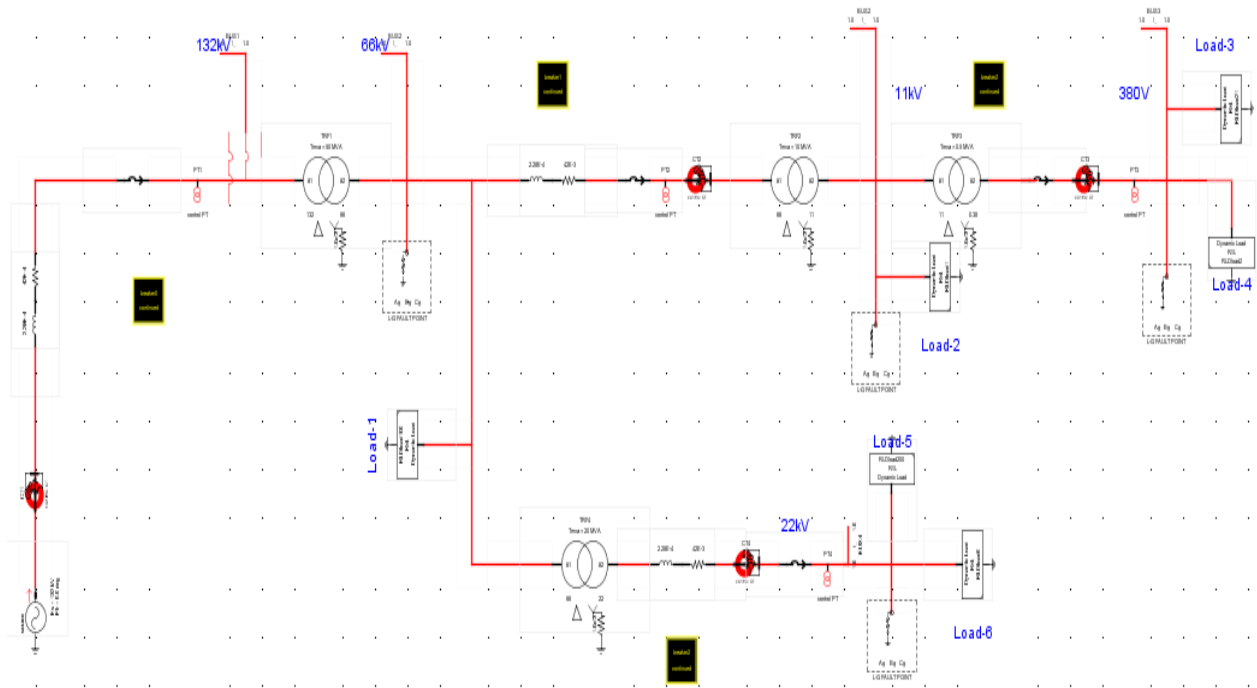


Figure 42: Distribution System Model on RSCAD environment

Dialing outputs that allow activation of fault using a push button, selection and alteration between the different combinations of line to ground faults via a dial switch.

Table 7: Dial output and corresponding fault

DIAL OUTPUT	BINARY OUTPUT	FAULT APPLIED
1	001	A-G
2	010	B-G
3	011	AB-G
4	100	C-G
5	101	AC-G
6	110	BC-G
7	111	ABC-G

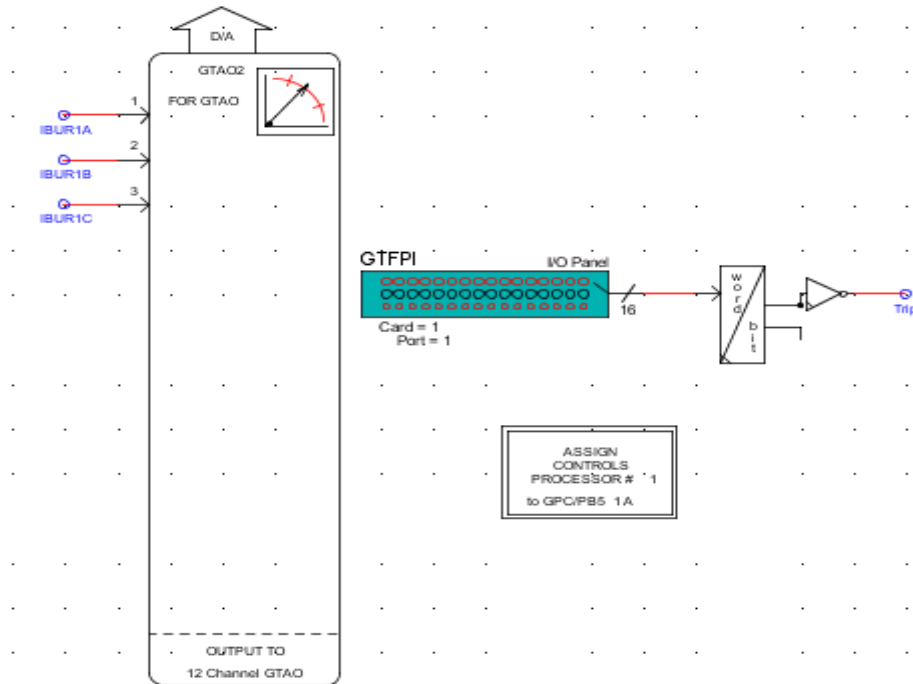


Figure 43: GTFPI and GTAO card used for exporting signals

B. Photovoltaic Generation Systems:

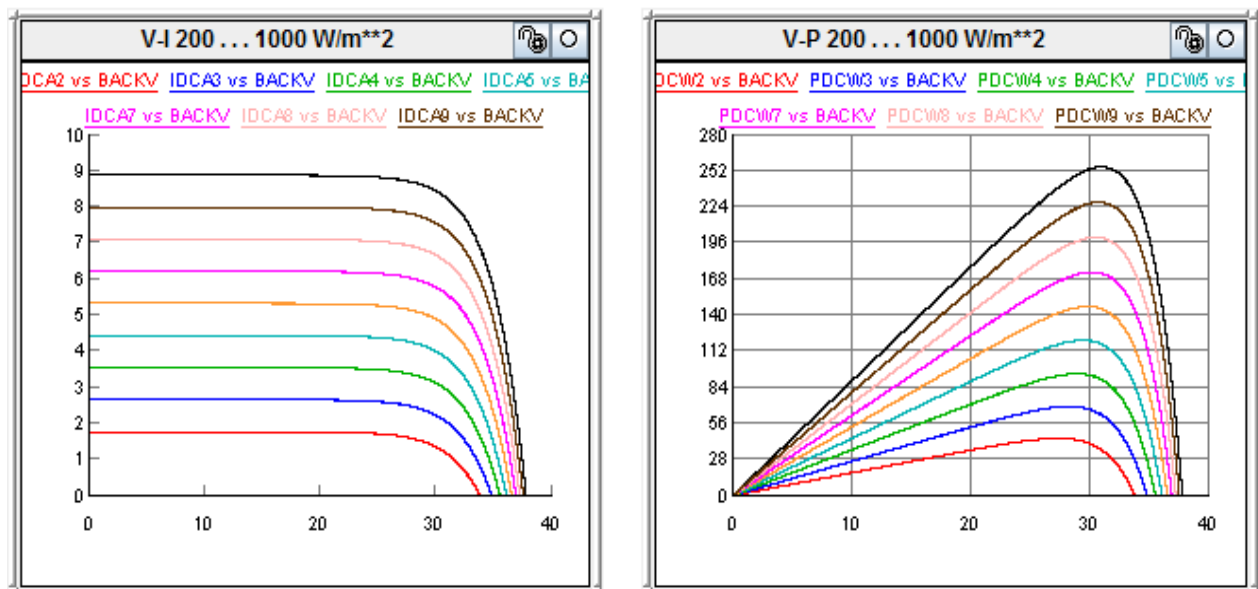


Figure 44: PV System characteristics graphs

A PV system MPPT controller:

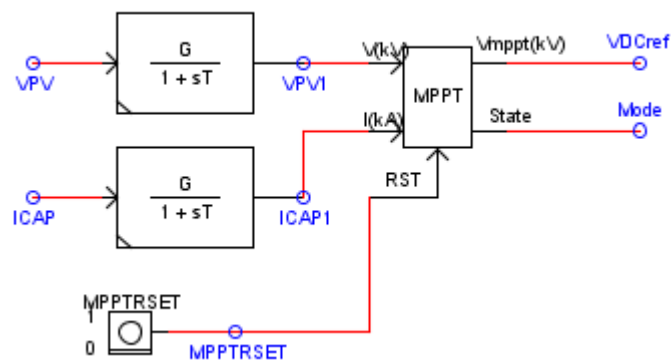


Figure 45: Maximum Power Point Tracking control circuit

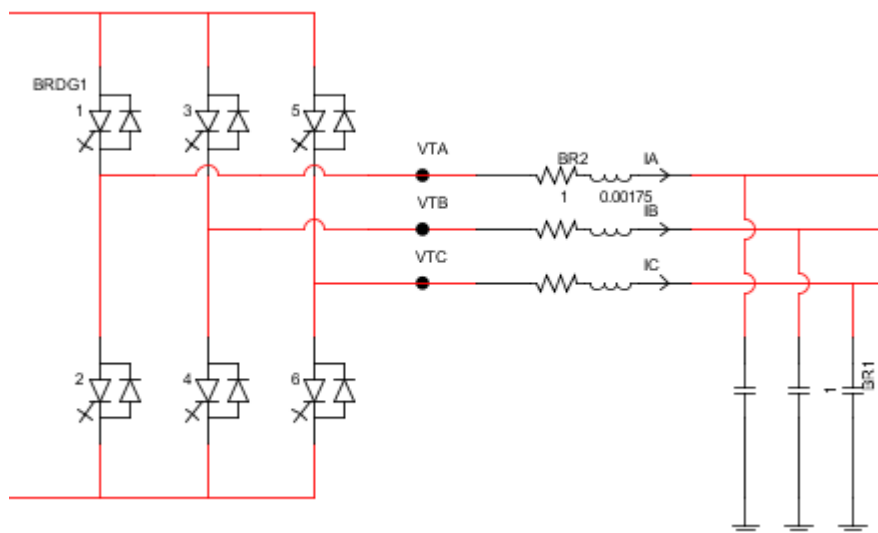


Figure 46: 2-level DC/AC inverter and filter

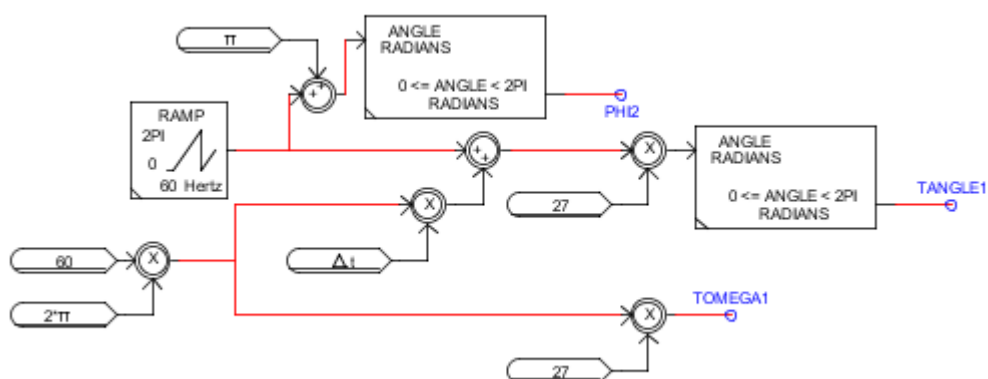


Figure 47: Triangle wave data generator for the DC/AC inverter

C. Grid-tied inverter System:

Dual simplex method iterations:

Table 8: 1st iteration (Slack variables as basics)

Basics	X_1	X_2	X_3	$S1$	$S2$	$S3$	$S4$	$S5$	B
$S1$	-1.43	1.29	0	1	0	0	0	0	-0.4
$S2$	0	-2.88	0.956	0	1	0	0	0	-0.4
$S3$	-1.6	0	0	0	0	1	0	0	-0.02
$S4$	0	-1.29	0	0	0	0	1	0	-0.02
$S5$	0	0	-0.956	0	0	0	0	1	-0.02

Table 9: 2nd iteration (X_2 enters as basic, $S2$ comes out)

Basics	X_1	X_2	X_3	$S1$	$S2$	$S3$	$S4$	$S5$	B
$S1$	-1.43	0	0.447	1	-1.29	0	0	0	-0.578
X_2	0	1	-0.347	0	1	0	0	0	0.138
$S3$	-1.6	0	0	0	0	1	0	0	-0.02
$S4$	0	0	-0.447	0	1.29	0	1	0	0.158
$S5$	0	0	-0.956	0	0	0	0	1	-0.02

Table 10: 3rd iteration (X_1 enters as basic, $S1$ comes out)

Basics	X_1	X_2	X_3	$S1$	$S2$	$S3$	$S4$	$S5$	B
X_1	1	0	-0.312	-0.699	0.90	0	0	0	0.404
X_2	0	1	-0.347	0	1	0	0	0	0.138
$S3$	0	0	-0.5	-1.12	1.44	1	0	0	0.626
$S4$	0	0	-0.447	0	1.29	0	1	0	0.158
$S5$	0	0	-0.956	0	0	0	0	1	-0.02

Table 11: 4th iteration (X_3 enters as basic, $S5$ comes out)

Basics	X_1	X_2	X_3	$S1$	$S2$	$S3$	$S4$	$S5$	B
X_1	1	0	0	-0.699	0.90	0	0	0	0.41
X_2	0	1	0	0	1	0	0	0	0.145
$S3$	0	0	0	-1.12	1.44	1	0	0	0.636
$S4$	0	0	0	0	1.29	0	1	-0.046	0.166
X_3	0	0	1	0	0	0	0	-1.04	0.021

